INFN
LNS
Istituto Nazionale di Fisica Nucleare
Laboratori Nazionali del Sud

Co-propagating Dielectric Laser Accelerators for compact high-gradient particle acceleration

Giuseppe Torrisi • *INFN–LNS, Catania, Italy*

G. S. Mauro, D. Mascali ***(INFN-LNS),*** A. Bacci ***(INFN-Milano)***
R. Palmeri ***(UniRC)***, A. Locatelli ***(UniBS)***, L. Vincetti ***(UniMoRe)***, G. Sorbello ***(UniCT)***

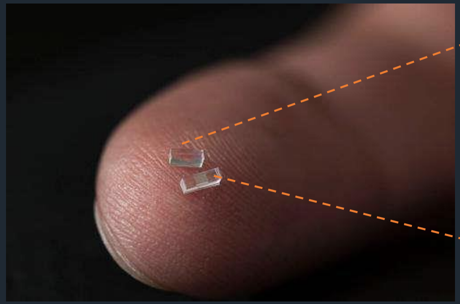

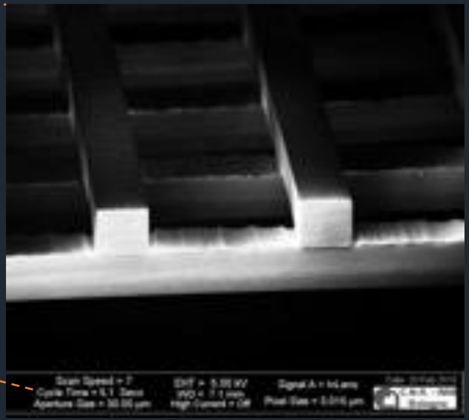

A Roadmap Toward Scalable Dielectric Laser Acceleration

Scalable dielectric laser acceleration relies on
co-propagating waveguide structures, phase synchronism, and integrated EM–beam dynamics co-design.
Together, they provide a pathway toward scalable particle acceleration.

1 Phase synchronism

while β increases

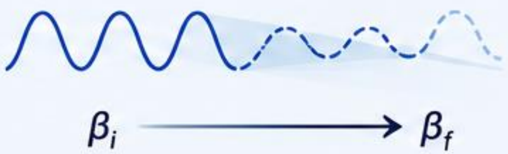

Maintain phase synchronism as the particle velocity increases.

→

2 Co-propagating guided interaction

scalable to long interaction lengths

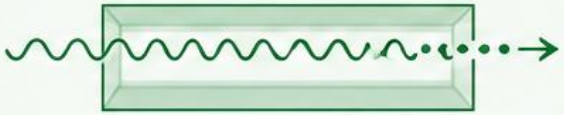

Enable strong, efficient laser–particle interaction over increasing distances.

→

3 Stepwise experimental validation

from optical metrology to particle acceleration

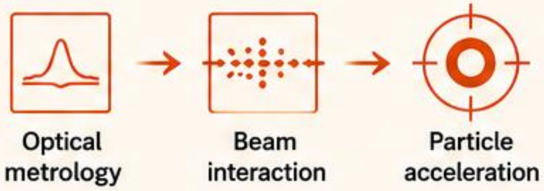

Validate performance through a progressive experimental path.

This talk focuses primarily on the first two challenges:
phase synchronism and co-propagating guided interaction.

Why co-propagating DLA?

RF / microwave

10–100 MV/m
large cavities

→

Optical DLA

GV/m fields
micro/nano structures

- **micro/nano-fabricated "chip-scale" Dielectric *(typically silicon)* Acceleration structures**
- **conventional** ultrafast ***(fs)* infrared *(1-5 μm)* lasers *(solid state)***
- **accelerating gradient up to 2 orders of magnitude greater conventional RF accelerators**.

Cross-propagating architectures have demonstrated DLA physics, but extending the interaction or staging many periods requires increasingly complex side power-delivery networks.

Co-propagating guided structures offer a quasi-1D scaling path: the optical mode and the particle beam share the same axis enabling a travelling-wave-like interaction

Dielectric Laser Guiding strategies

Cross-propagating / side-pumped

- *Inverse Smith–Purcell*
- *Inverse Cherenkov*
- *Dual-grating with PFT / SLM*

Strength: ✔ experimental maturity
Challenge: scaling interaction length

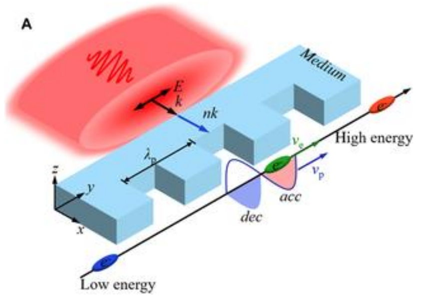

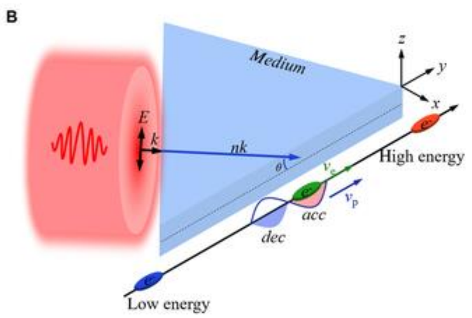

Co-propagating / guided

(This Talk)

- *Slot Waveguides*
- *Hollow-core photonic crystals*
- *Hybrid phase-matched structures*

Strength: natural scalabity
Challenge: experimental validation
phase and group velocity control
fabrication tolerances

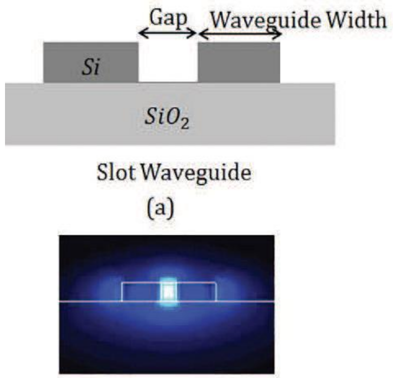

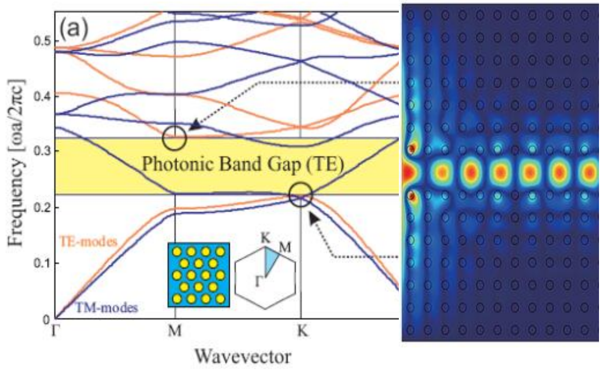

From AAC 2024 to AAC 2026

The previous WG4 summary defines the scaling problem we want to address.

AAC 2024 WG4 identified

- interaction-length limitation
- longitudinal/transverse beam dynamics
- phase and group-velocity control

[G. Andonian and E. Snively, "Summary of Working Group 4: Novel Structure Acceleration," NIM A 1072, 170132 (2025)]

Our work

- co-propagating guided modes
- slot + suspended slot • hollow-core PhC structures
- geometry-controlled phase velocity;

From peak gradient → controlled, extended and scalable energy gain

State of the Art of Dielectric Laser Acceleration

2013 First acceleration
↓
2018 Sub-relativistic DLA
↓
2024–26 Programmable optics (mm interaction)

Scheme	Beam	Gradient	Length	ΔE	Charge	Ref.
ISP (rel.)	Rel. (MeV beam)	0.3–0.8 GV/m	10–100 μm	~10–100 keV	fC	Cesar et al., 2018
Dual grating + PFT	Rel. (UCLA linac)	~0.5 GV/m	0.5–1 mm	~100–300 keV	fC	Cesar et al., 2018; Crisp et al., 2024
Inverse Cherenkov	Rel. (MeV beam)	>1.6 GV/m	0.1–0.3 mm	~100 keV	fC	Breuer & Hommelhoff, 2013
On-chip photonics	Sub-rel. (keV beam)	~1–2 GV/m	50–200 μm	~10–50 keV	sub-fC	Sapra et al., 2020; Nature 2024
APF structures	Sub-rel. (keV beam)	30–50 MeV/m	~0.7 mm	~keV	fC	Niedermayer et al., 2018
Slot waveguide (Theory + numerical tracking)	Sub-rel. (keV beam)	333 MV/m (Predicted)	30 μm	10 keV		Zhao et al., Opt. Express 26 2018

State of the Art of Dielectric Laser Acceleration

2013 First acceleration
↓
2018 Sub-relativistic DLA
↓
2024–26 Programmable optics (mm interaction)

Scheme	Beam	Gradient	Length	ΔE	Charge	Ref.
ISP (rel.)	Rel. (MeV beam)	0.3–0.8 GV/m	10–100 μm	~10–100 keV	fC	Cesar et al., 2018
Dual grating + PFT+**SLM**	Rel. (UCLA linac)	~0.5 GV/m	0.5–**5 mm**	~100–500 keV	fC	Cesar et al., 2018; Crisp et al., 2024 **Crisp, et al., Nature Comm., in press (2026)**
Inverse Cherenkov	Rel. (MeV beam)	>1.6 GV/m	0.1–0.3 mm	~100 keV	fC	Breuer & Hommelhoff, 2013
On-chip photonics	Sub-rel. (keV beam)	~1–2 GV/m	50–200 μm	~10–50 keV	sub-fC	Sapra et al., 2020; Nature 2024
APF structures	Sub-rel. (keV beam)	30–50 MeV/m	~0.7 mm	~keV	fC	Niedermayer et al., 2018
Slot waveguide (Theory + numerical tracking)	Sub-rel. (keV beam)	333 MV/m (Predicted)	30 μm	**Starting point for our work**		**Zhao et al., Opt. Express 26 2018**

Programmable Optics + Structure-Based Phase Control?

Programmable optical control

control applied to the drive laser

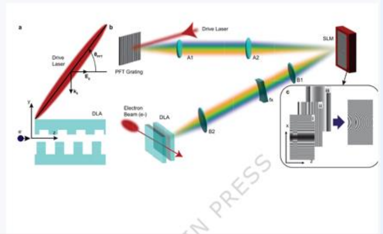

S. Crisp, R. J. England, A. Ody, P. Musumeci, Nature Communications, in press (2026)

UCLA/SLAC benchmark

- ✓ >4 mm phase-matched interaction
- ✓ up to 0.55 ± 0.05 MeV energy gain
- ✓ phase / amplitude shaping with PFT + SLM

+

control layer

Structure-based phase control

control embedded in the guided eigenmode

laser mode + electron beam share the same axis

- ✓ Co-propagating guided modes
- ✓ Geometry-tuned phase velocity
- ✓ Integrated EM–beam-dynamics co-design

route investigated in this work

Programmable optics controls the drive; structural engineering controls the guided mode.

A multi-stage velocity-matched architecture

Different photonic platforms can cover different β-ranges and be cascaded.

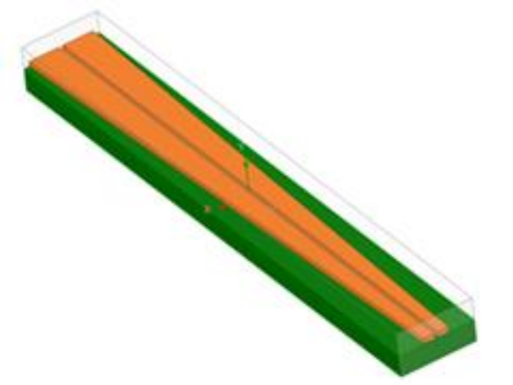

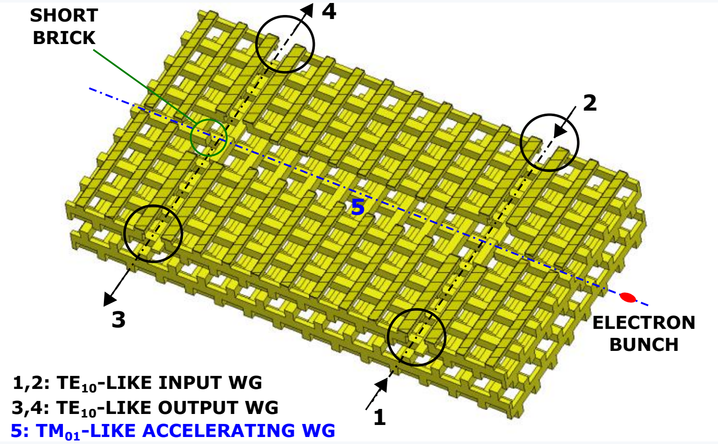

Tapered suspended slot → **Hollow-core PhC taper** → **Relativistic module / woodpile**

β ≈ 0.4–0.65

β ≈ 0.7–1

β ≈ 1

Design principle: adapt the photonic environment so that the guided mode remains synchronous with the accelerating particle.

[R. Palmeri et al., Opt. Express 31, (2023)]
[R. Palmeri et al., IEEE Photon. Technol. Letters, 38, 7, (2026)]
[D. Guarnera et al., EuCAP, 2025]

[G. Torrisi et al., IEEE MWCL, 30, 4, (2020)]
[G. S. Mauro et al., IEEE MTT, 68, 5, (2020)]
[G.S. Mauro et al., M Opt Tech Lett. (2019)]

A multi-stage velocity-matched architecture

Different photonic platforms can cover different β-ranges and be cascaded.

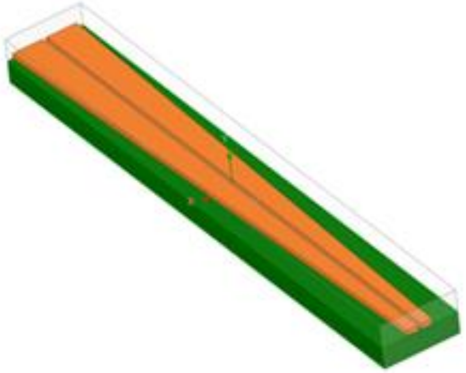

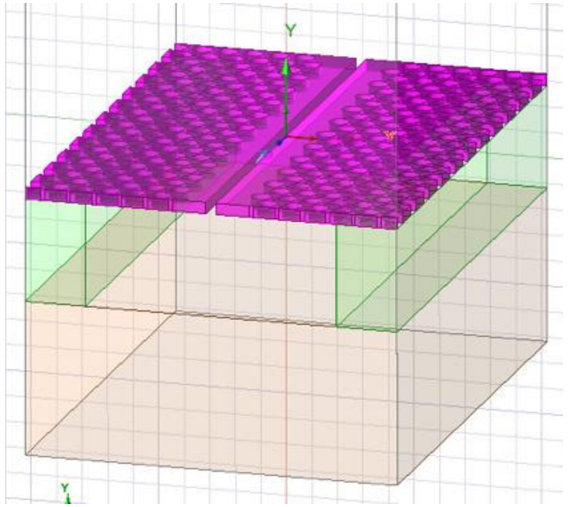

Tapered suspended slot

Hollow-core PhC taper

hybrid structure: photonic-slot waveguide

$\beta \approx 0.4–0.65$

$\beta \approx 0.7–1$

$\beta \approx 1$

Design principle: adapt the photonic environment so that the guided mode remains synchronous with the accelerating particle.

Part I — Slot waveguides

slot waveguide design: geometry

- High-index strips separated by a small gap
- Selective excitation of the accelerating mode
- Tuning of cross section to synchronize <u>sub-relativistic</u> particles

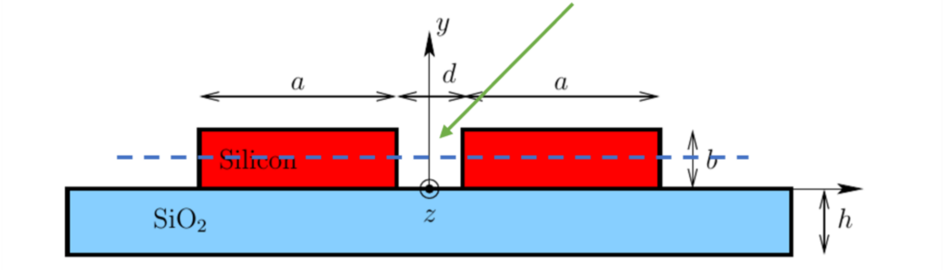

"Fundamental" mode - electric field
Ez component (even symmetry)

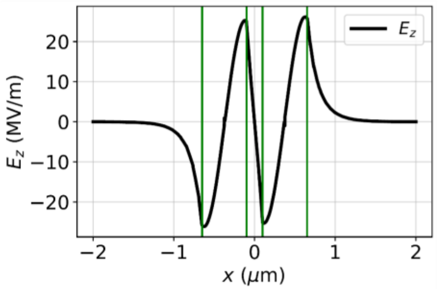

"Accelerating" mode - electric field
Ez component (odd symmetry)

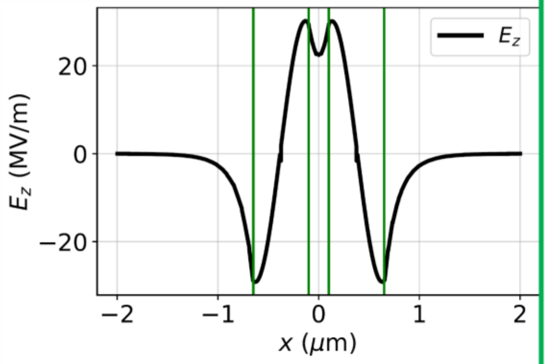

Schematic of a slot waveguide

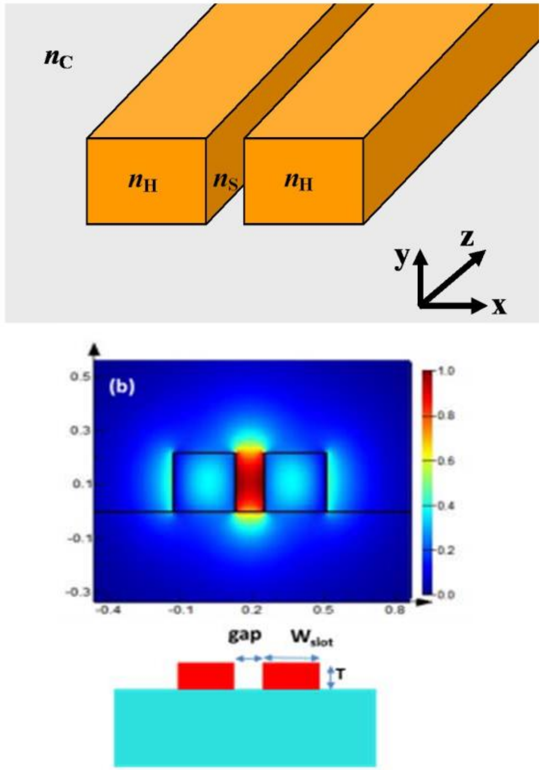

Accelerating slot waveguide design

Synchronicity

For a varying particle velocity, we need a non-uniform slot waveguide

Electron traveling with velocity $v_e(z)$

$$\Delta W = -eE_0 \int_0^{L_{acc}} \cos\left[\omega\left(t_0 + \int_0^z \frac{dz'}{v_e(z')} - \int_0^z \frac{dz'}{v_\phi(z')}\right) + \phi_0\right] dz$$

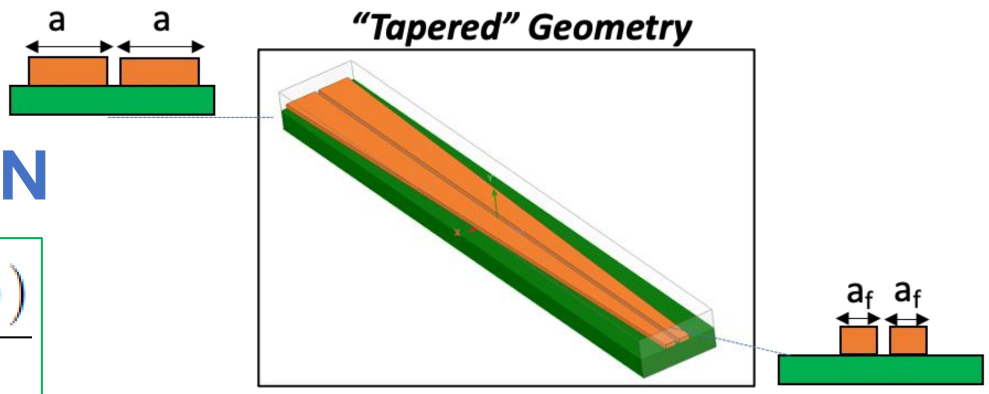

non-uniform slot waveguide

SYNCHRONOUS CONDITION

$$\frac{v_e(z)}{c} = \beta_e(z) = \beta_\phi(a(z)) = \frac{v_\phi(a(z))}{c}$$

$$a = a(z) \quad \text{s.t.} \quad \beta_\phi(a(z)) = \beta_e(z)$$

Physics-based design steps

- **Slot waveguide [0.4<β<0.65]**

STEP 1: Relativistic dynamic evaluation

$$\Delta W = q\int_0^L E_z(z,t)dz = q\int_0^L E_0 \cos\left\{ \omega\left[\int_0^z \frac{1}{v_{\text{part}}(z')}dz' - \int_0^z \frac{1}{v_{\text{ph}}(z')}dz'\right]\right\} dz$$

=1 for ΔW maximization

$E(z,t)=E_0$ @ 1st STEP 1

$$\begin{cases} \frac{dp}{dt} = qE(z,t) \\ \frac{dz}{dt} = \frac{p}{\sqrt{\frac{p^2}{c^2}+m_0^2}} \end{cases} \rightarrow p(z,t) \rightarrow v$$

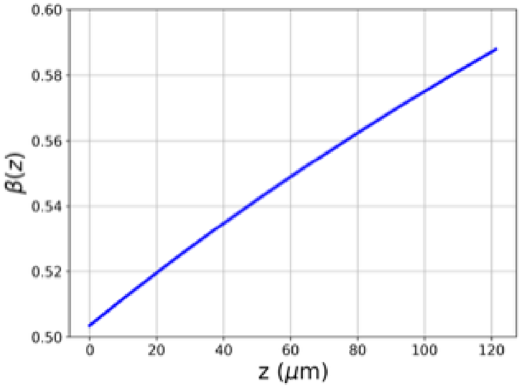

Theoretical ideal BD result

Physics-based design steps

- **Slot waveguide [0.4<β<0.65]**

STEP 1: Relativistic dynamic evaluation

$$\Delta W = q\int_0^L E_z(z,t)dz = q\int_0^L E_0 \cos\left\{ \omega\left[\int_0^z \frac{1}{v_{\text{part}}(z')}dz' - \int_0^z \frac{1}{v_{\text{ph}}(z')}dz'\right]\right\} dz$$

=1 for ΔW maximization

E(z,t)=E$_0$ @ 1st STEP 1

$$\begin{cases} \dfrac{dp}{dt} = qE(z,t) \\ \dfrac{dz}{dt} = \dfrac{p}{\sqrt{\frac{p^2}{c^2}+m_0^2}} \end{cases} \rightarrow p(z,t) \rightarrow v$$

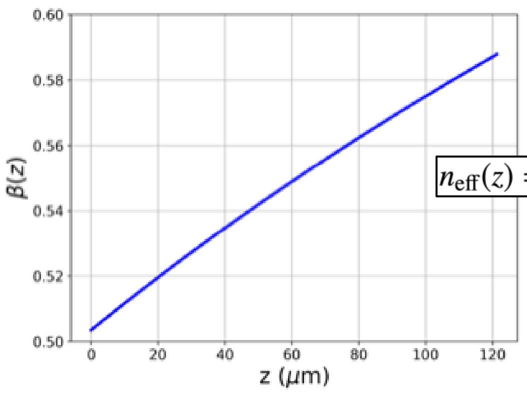

Theoretical ideal BD result

$n_{\text{eff}}(z) = 1/\beta(z)$

STEP 2: Derivation of a calibration curve $\beta(z) \rightarrow n_{eff}(z) \rightarrow a(z)$

parametric study in COMSOL

Calibration Curve

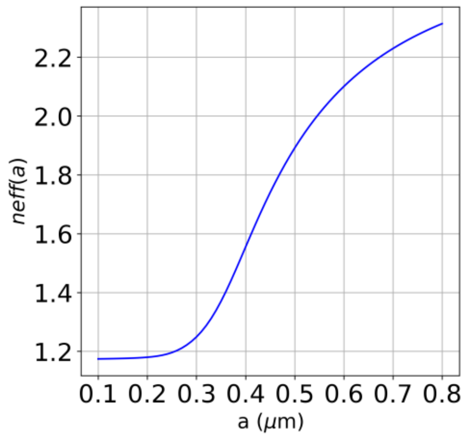

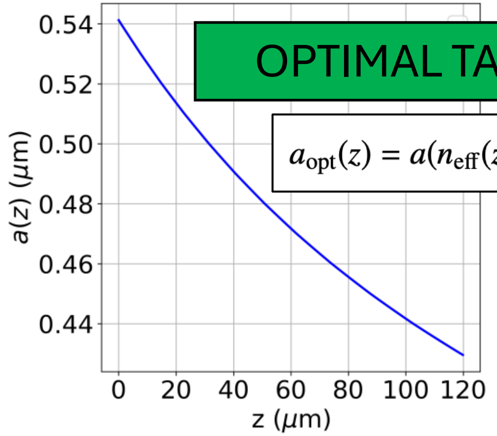

OPTIMAL TAPER

$a_{\text{opt}}(z) = a(n_{\text{eff}}(z)) = a(\beta(z))$

Physics-based design steps

- **Slot waveguide [0.4<β<0.65]**

STEP 1: Relativistic dynamic evaluation

$$\Delta W = q\int_0^L E_z(z,t)dz = q\int_0^L E_0 \cos\left\{\ \omega\left[\int_0^z \frac{1}{v_{\text{part}}(z')}dz' - \int_0^z \frac{1}{v_{\text{ph}}(z')}dz'\right]\ \right\} dz$$

=1 for ΔW maximization

$E(z,t)=E_0$ @ 1st STEP 1

$$\begin{cases} \frac{dp}{dt} = qE(z,t) \\ \frac{dz}{dt} = \frac{p}{\sqrt{\frac{p^2}{c^2}+m_0^2}} \end{cases} \rightarrow p(z,t) \rightarrow v$$

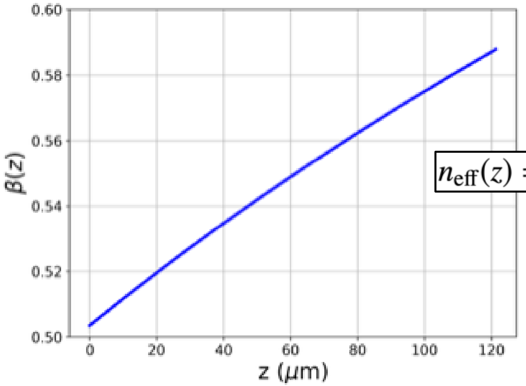

Theoretical ideal BD result

$n_{\text{eff}}(z) = 1/\beta(z)$

STEP 2: Derivation of a calibration curve

$\beta(z) \rightarrow n_{eff}(z) \rightarrow a(z)$

parametric study in COMSOL

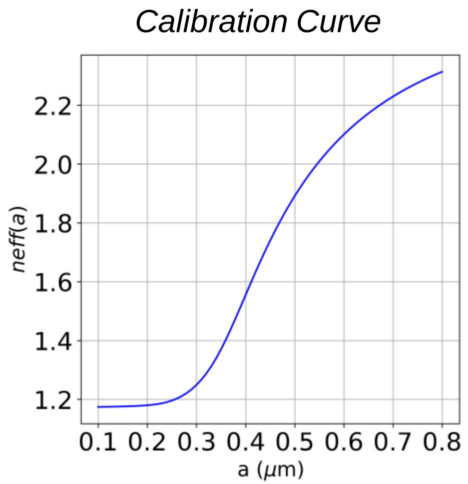

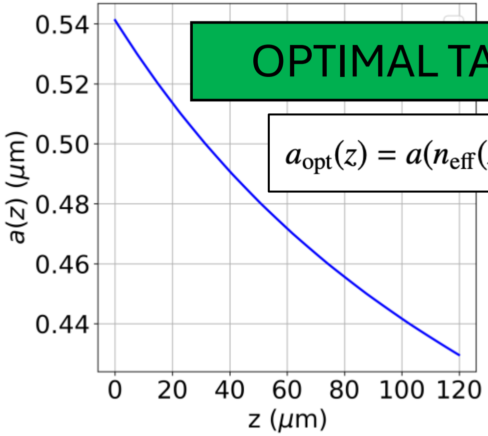

OPTIMAL TAPER

$a_{\text{opt}}(z) = a(n_{\text{eff}}(z)) = a(\beta(z))$

$E(z,t)$

STEP 3: Testing of the taper (3D) through EM COMSOL simulation

Physics-based design steps

- **Slot waveguide [0.4<β<0.65]**

STEP 1: Relativistic dynamic evaluation

$$\Delta W = q\int_0^L E_z(z,t)dz = q\int_0^L E_0 \cos\left\{ \omega\left[\int_0^z \frac{1}{v_{\mathrm{part}}(z')}dz' - \int_0^z \frac{1}{v_{\mathrm{ph}}(z')}dz'\right]\right\} dz$$

=1 for ΔW maximization

$$\begin{cases} \dfrac{dp}{dt} = qE(z,t) \\ \dfrac{dz}{dt} = \dfrac{p}{\sqrt{\dfrac{p^2}{c^2}+m_0^2}} \end{cases}$$

$E(z,t)$

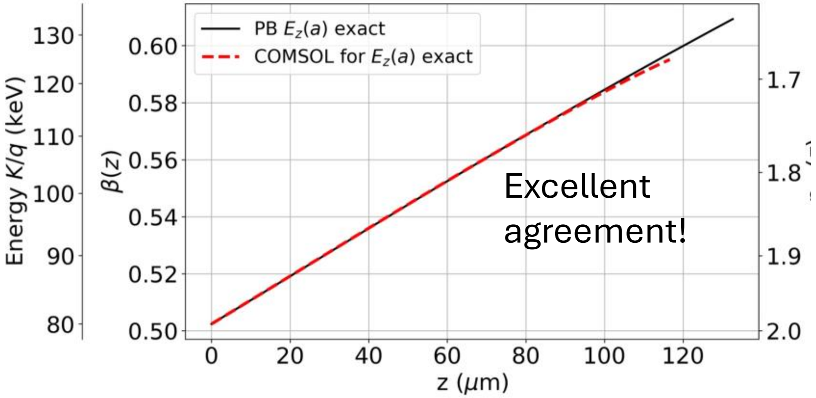

-Theoretical ideal
vs
---Numerical
BD result

STEP 2: Derivation of a calibration curve
$\beta(z) \to n_{eff}(z) \to a(z)$

parametric study in COMSOL

Calibration Curve

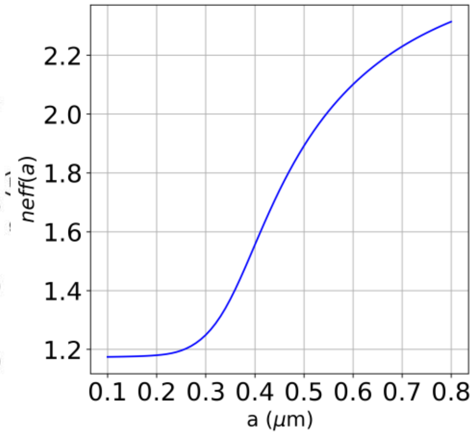

OPTIMAL TAPER

$a_{\mathrm{opt}}(z) = a(n_{\mathrm{eff}}(z)) = a(\beta(z))$

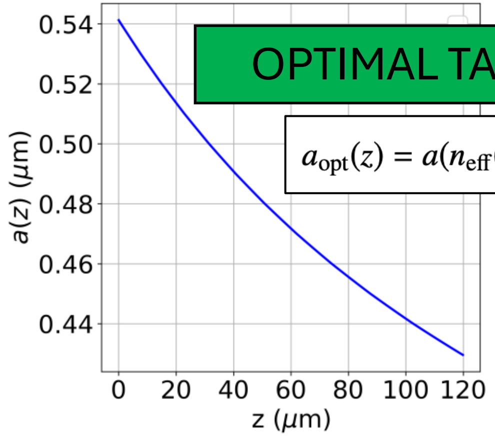

STEP 3: Testing of the taper (3D) through EM COMSOL simulation

What happens for a uniform (NON-TAPERED) slot waveguide?

- **Slot waveguide [0.4<β<0.65]**

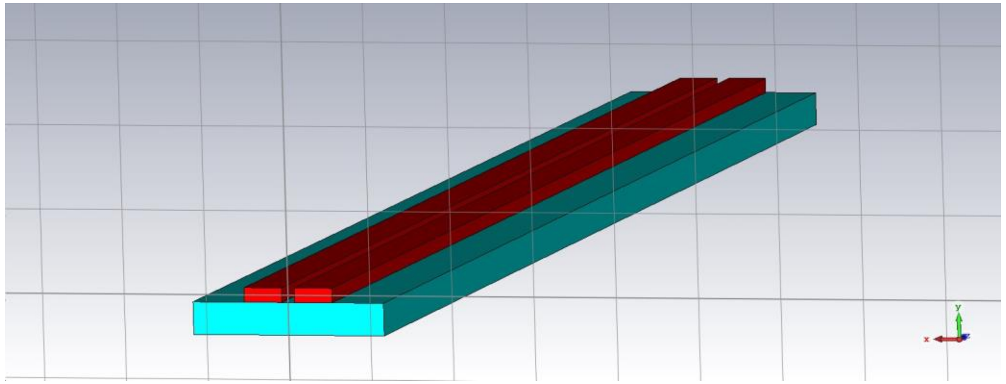

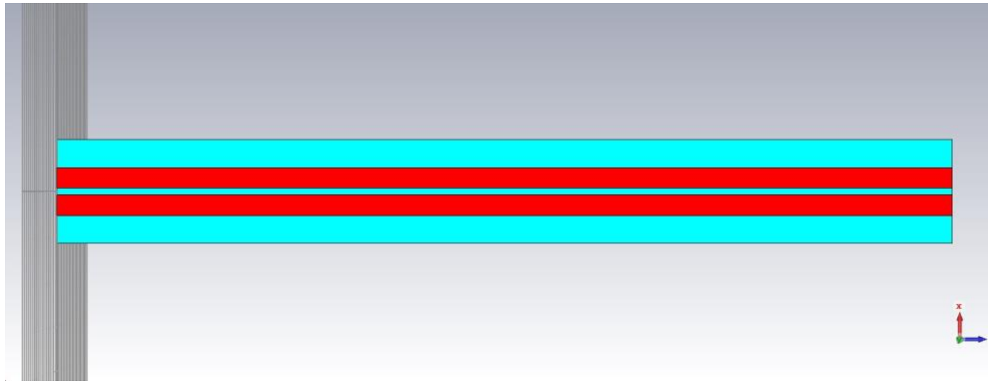

No particle in the accelerating RF bucket!

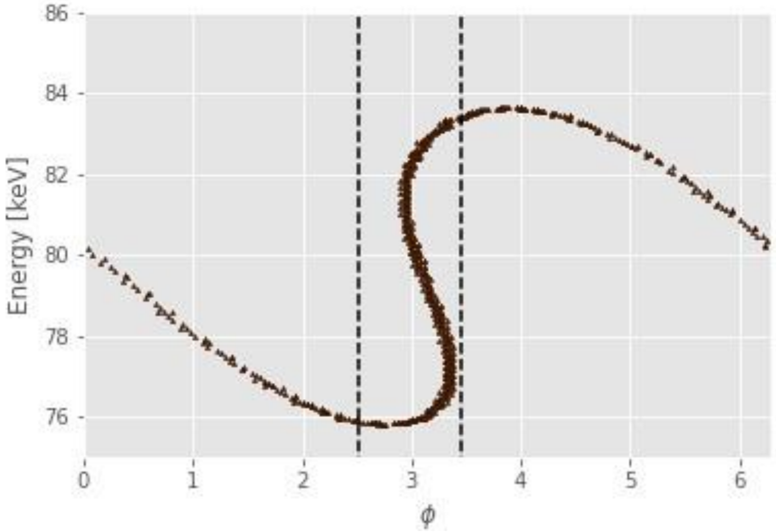

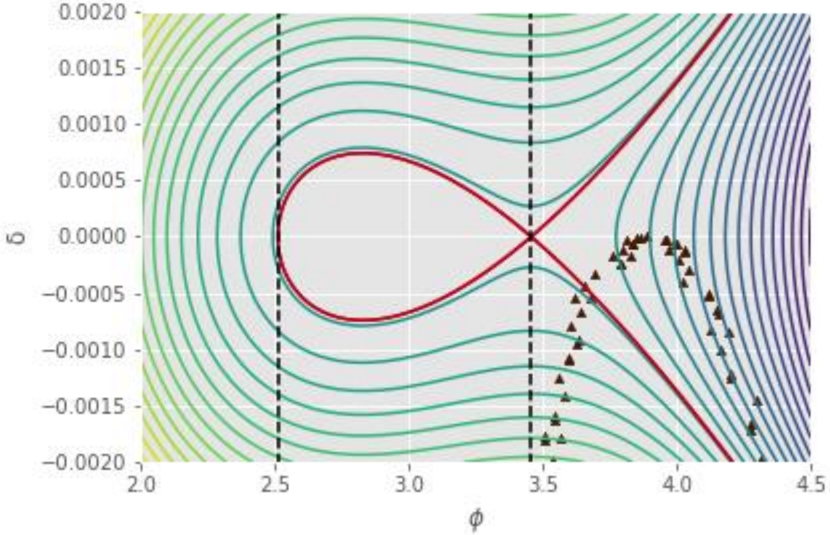

PHASE SPACE AT ACCELERATOR’S EXIT

- **Slot waveguide [0.4<β<0.65]**

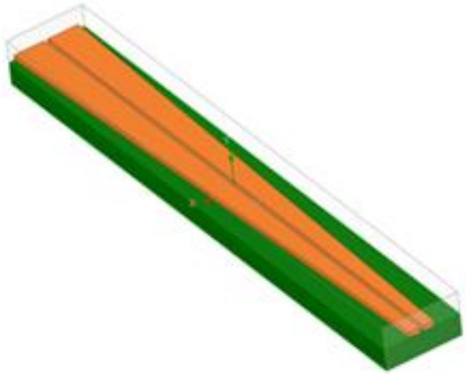

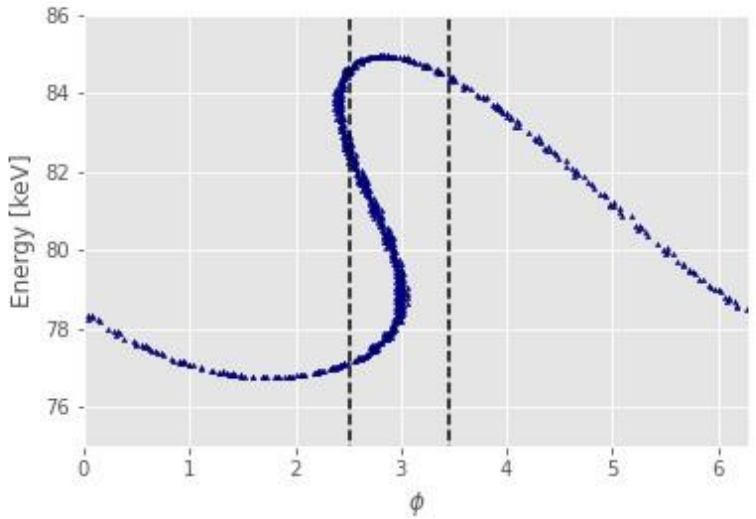

Electron phase space after acceleration.

High-density of points inside the separatrix.

electrons phase space

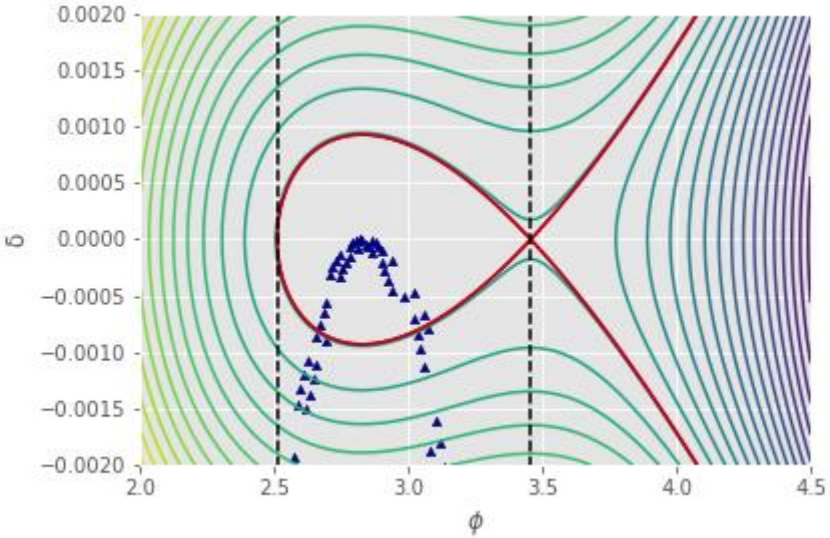

Performance comparison

- **Slot waveguide [0.4<β<0.65]**

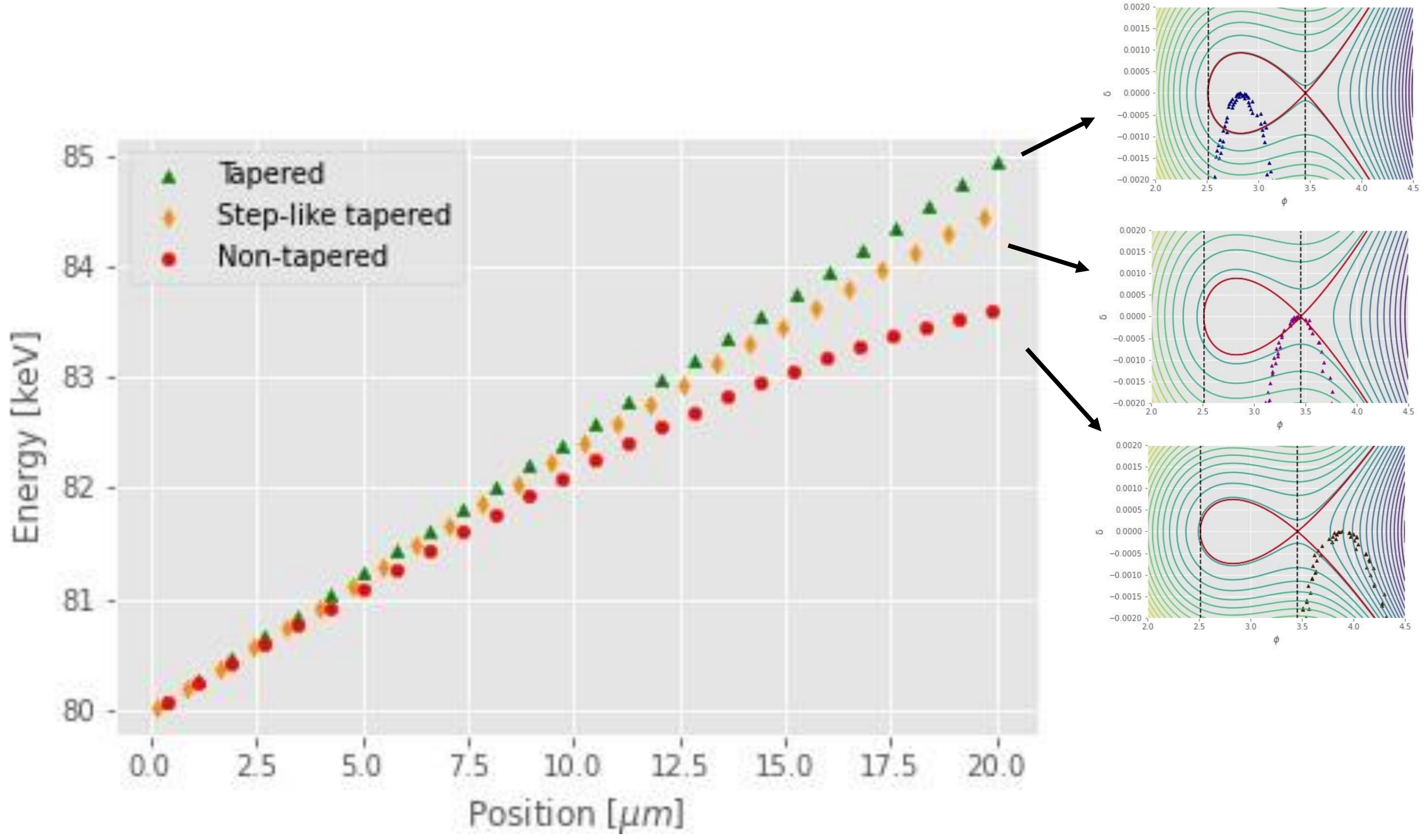

2D reduced model → enables rapid taper optimization before full 3D validation

The reduced model enables rapid design-space exploration.

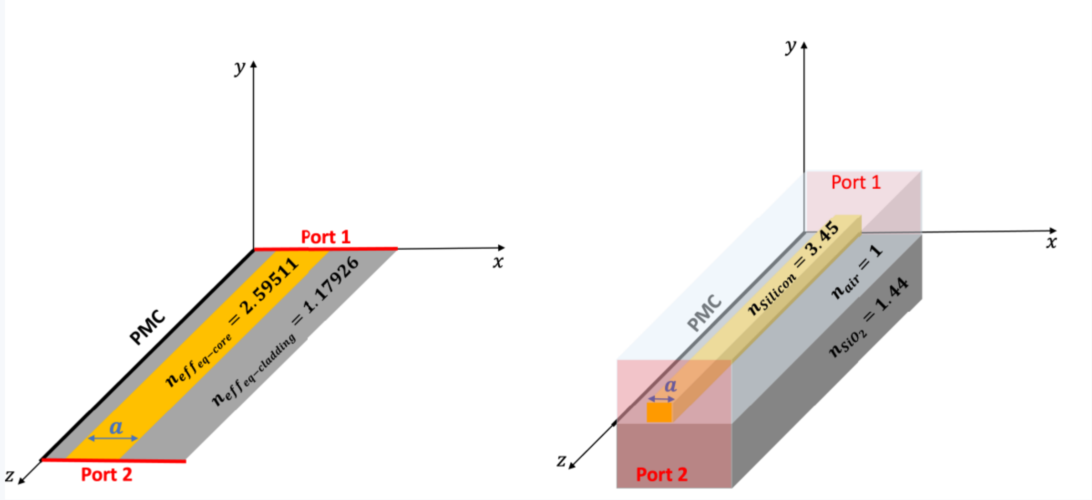

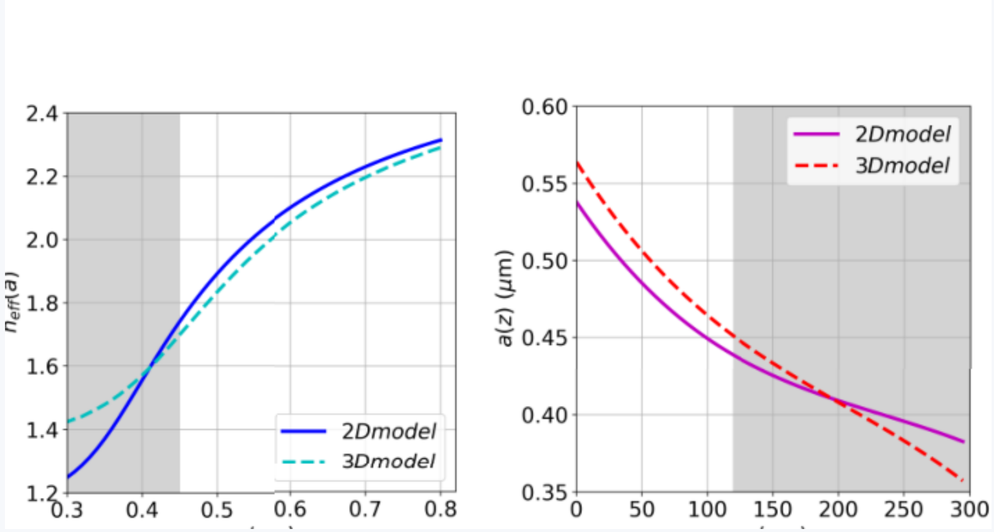

[R. Palmeri et al., Optics Express 31, 38891–38909 (2023).]

Nelder_Mead method optimization

(also called downhill simplex method)
algorithm used to find the optimum (minimum or maximum) of an objective function or a FoM in a multidimensional space

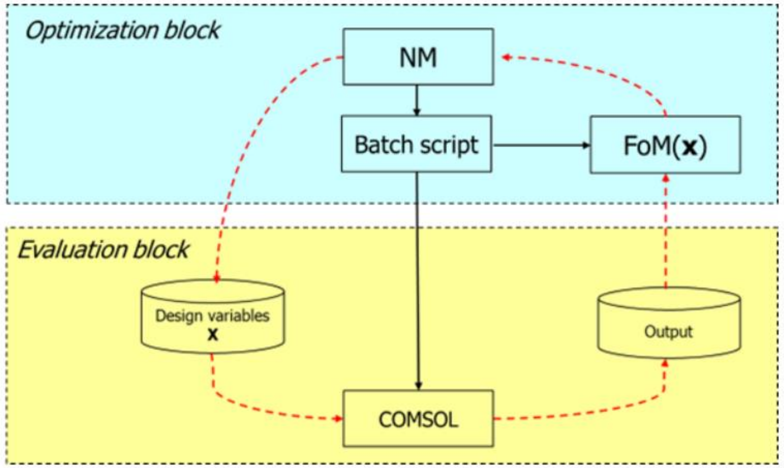

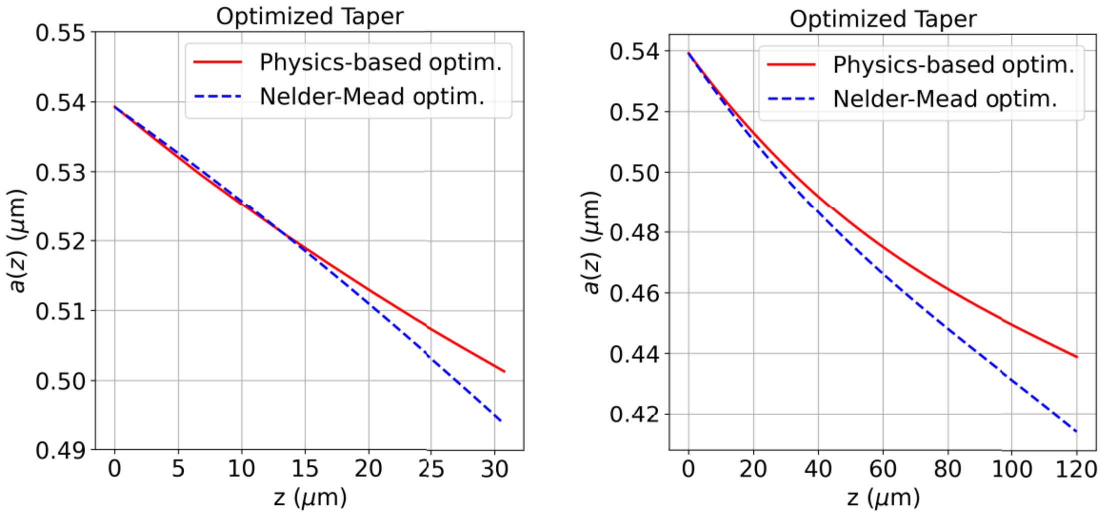

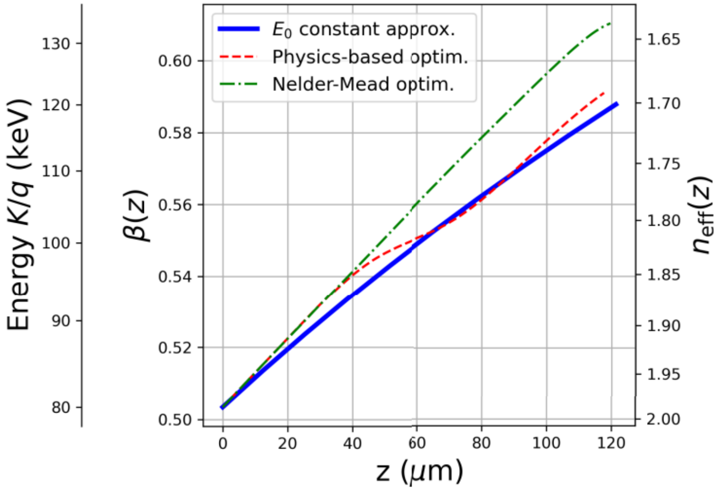

- a higher output energy
- more stable and monotonic acceleration

Suspended slot waveguide: extending the accessible β range

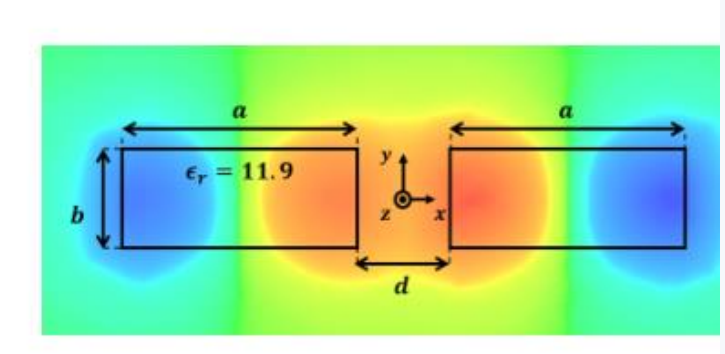

Cross-section overlaid with of E_z for the second (odd) mode

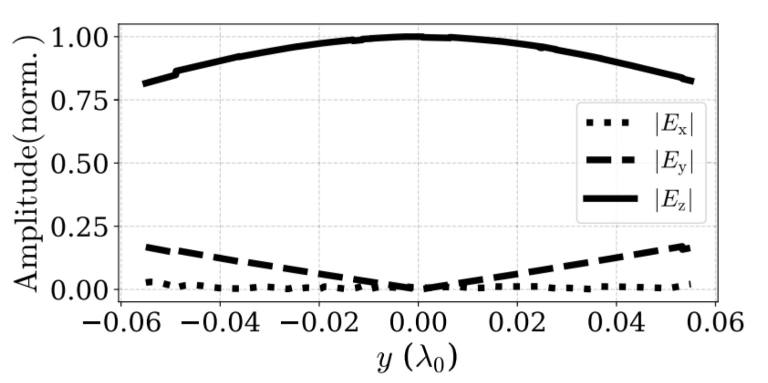

1D cut of the electric field component

Why suspended?

- no SiO_2 substrate losses
- vertical symmetry
- smaller transverse force components
- lower n_{eff} accessible → higher v_{ph}
- better compatibility with β increase

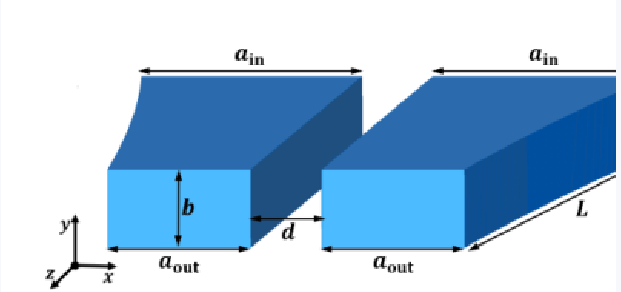

3D view of the designed suspended Slot waveguide

[R. Palmeri, G. Torrisi et al., IEEE Photonics Technology Letters 38(7), 475–478 (2026).]

Physics-assisted design: calibration curves drive the taper

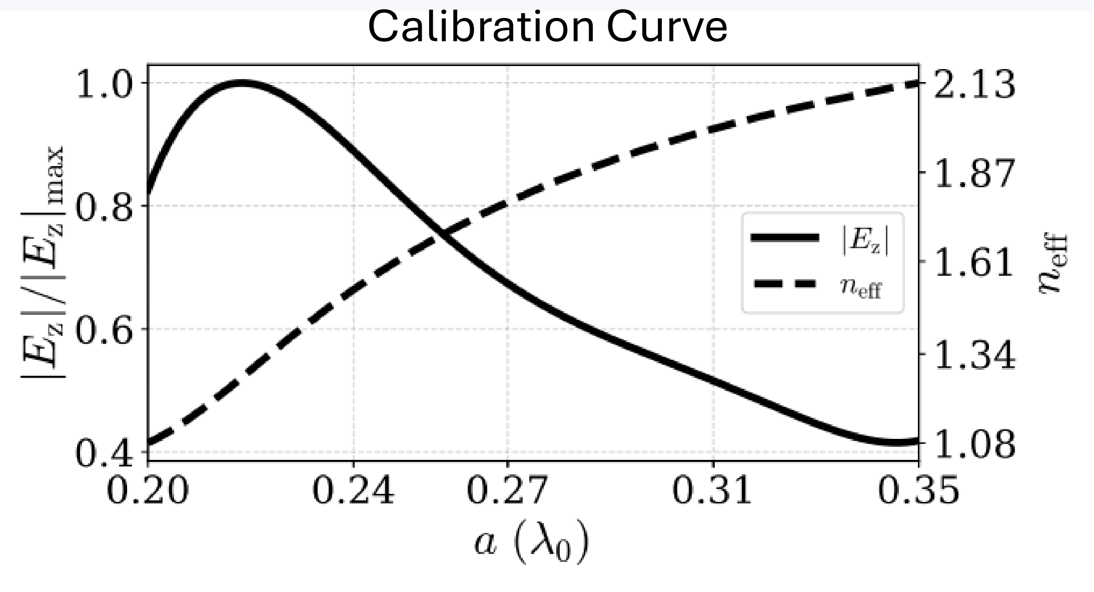

Improvement over the earlier model

The taper accounts not only for $n_{eff}(a)$, but also, for the slow variation of $E_z(a)$ along the structure.

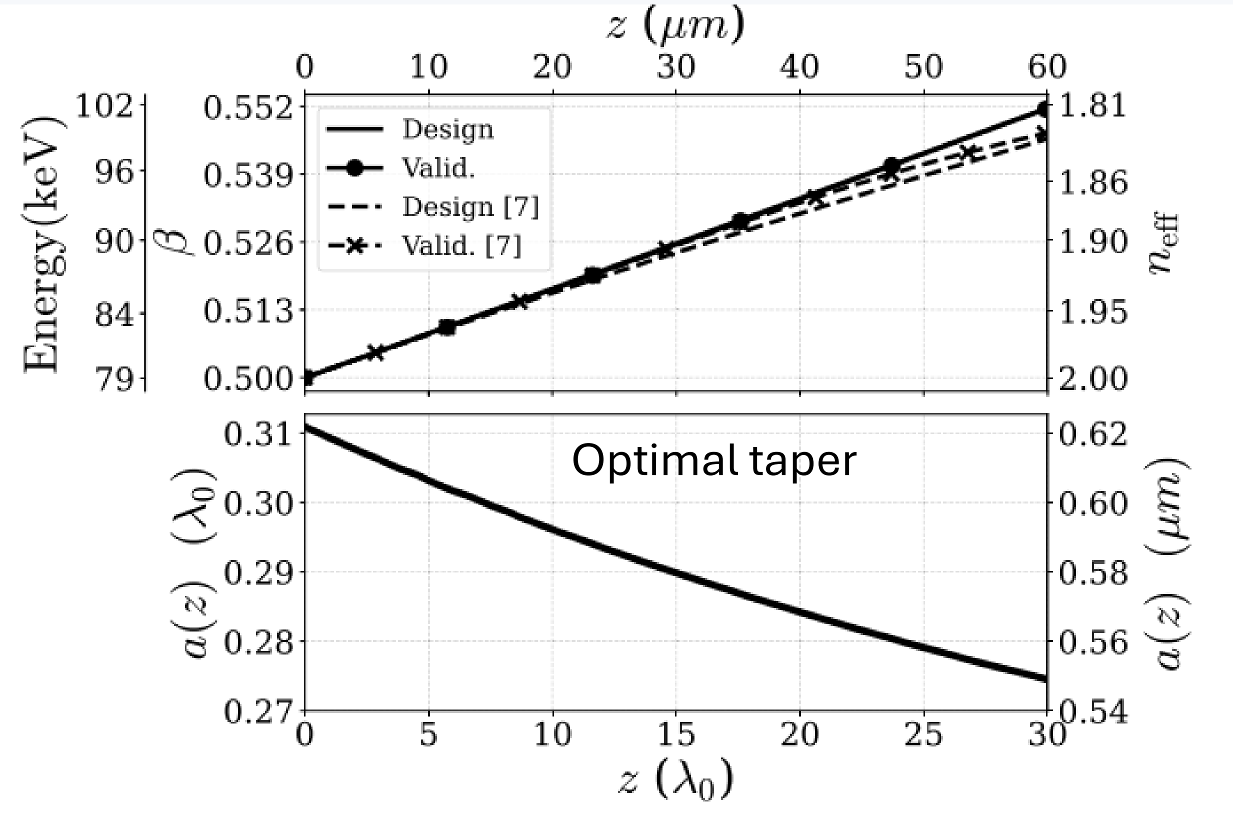

Physics-based optimization results with numerical validation and comparison to the previous approach

R. Palmeri et al., IEEE Photonics Technology Letters 38(7), 475–478 (2026).

Continuous acceleration with physics-designed suspended slot taper

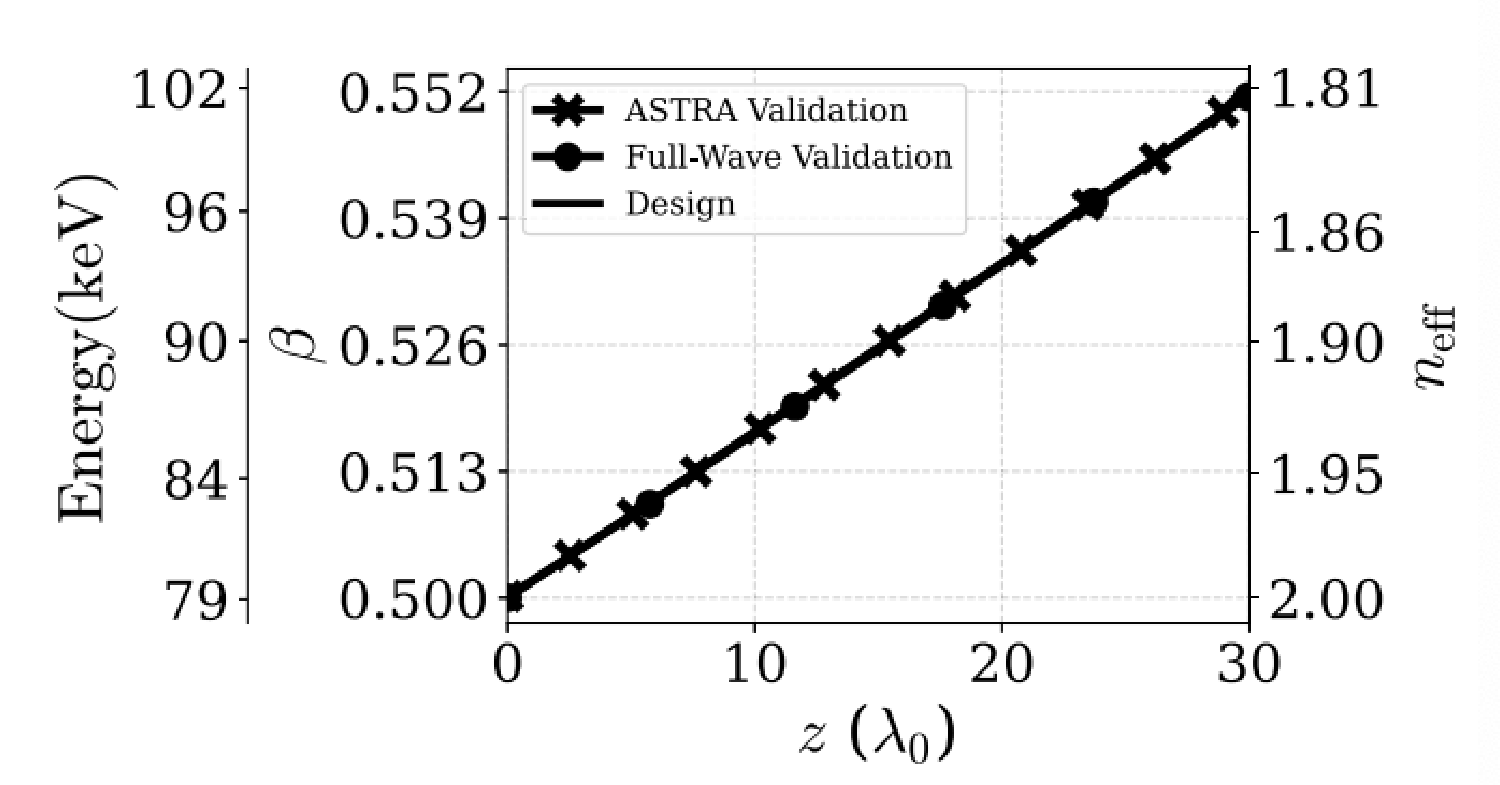

Continuous synchronism maintained

Key numbers

Input energy
79 keV

Output energy
102 keV

Net gain ≈ 23 keV
≈20% improvement vs constant-field model

EM fields: HFSS
Beam dynamics: ASTRA

New feature: unlike the 2023 model, the taper simultaneously accounts for phase velocity and local accelerating-field variation, leading to a self-consistent taper desig

Self-consistent physics-based taper design

The taper is determined by both phase synchronism and the local accelerating field.

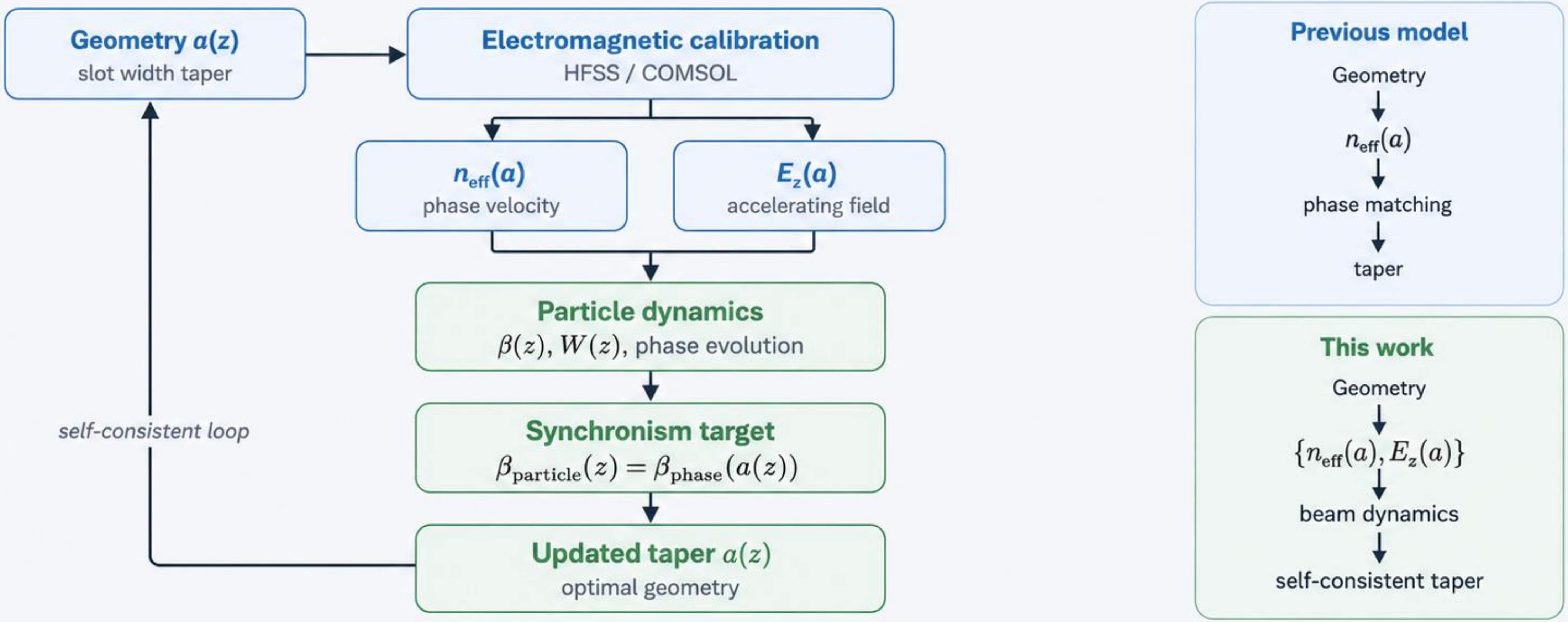

New ingredient: local EM calibration provides both phase velocity and accelerating-field amplitude, yielding a self-consistent taper.

R. Palmeri et al., IEEE Photonics Technology Letters 38(7), 475–478 (2026).

Part II — Pulsed operation

Under pulsed excitation, the structure is not designed from phase velocity alone: the pulse envelope and the particle are advanced together along z.

Under pulsed excitation, phase matching alone is not enough

The particle samples a moving envelope, not only a phase-matched carrier.

Carrier phase

$v_{ph}(z)$ must follow $v_{particle}(z)$

Envelope walk-off

$v_g \neq v_{particle}$
short pulses can outrun or lag the particle

Dispersion + taper

k_2, k_3 and field-amplitude changes reshape the pulse

Therefore, the taper must be co-determined with the actual pulse propagation and particle dynamics.

Self-consistent time-domain modeling

A fast BPM propagates the pulse envelope while particle dynamics updates the taper.

$$\frac{\partial A}{\partial z} = \alpha A - \frac{1}{v_g}\frac{\partial A}{\partial t} - \frac{jk_2}{2}\frac{\partial^2 A}{\partial t^2} - \frac{k_3}{6}\frac{\partial^3 A}{\partial t^3},$$

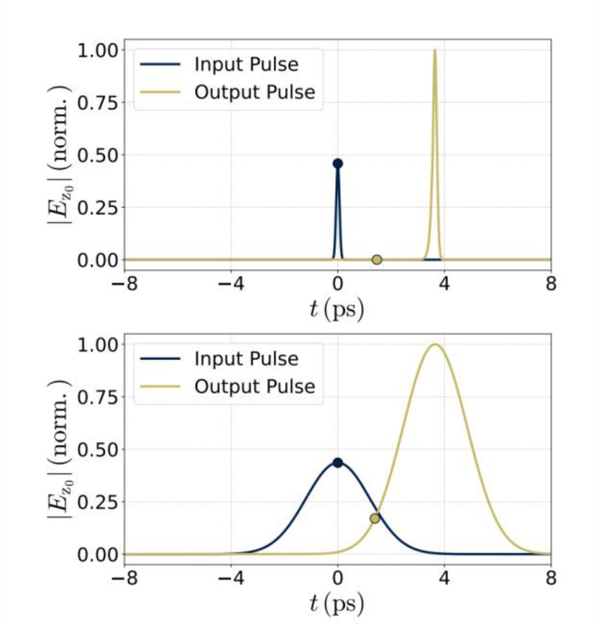

Model ingredients

- Beam Propagation Method for the pulse envelope
- local vg, k_2, k_3 from modal calibration
- taper-induced field-amplitude variation
- relativistic single-particle dynamics
- self-consistent update of a(z)

Current status: manuscript in preparation / internal validation.

D. Guarnera et al., “Self-Consistent Time-Domain Modeling of Pulsed Dielectric Laser Accelerators,” manuscript in preparation (2026).

Single pulses versus pulse trains

Pulse duration and pulse timing directly control the usable interaction length.

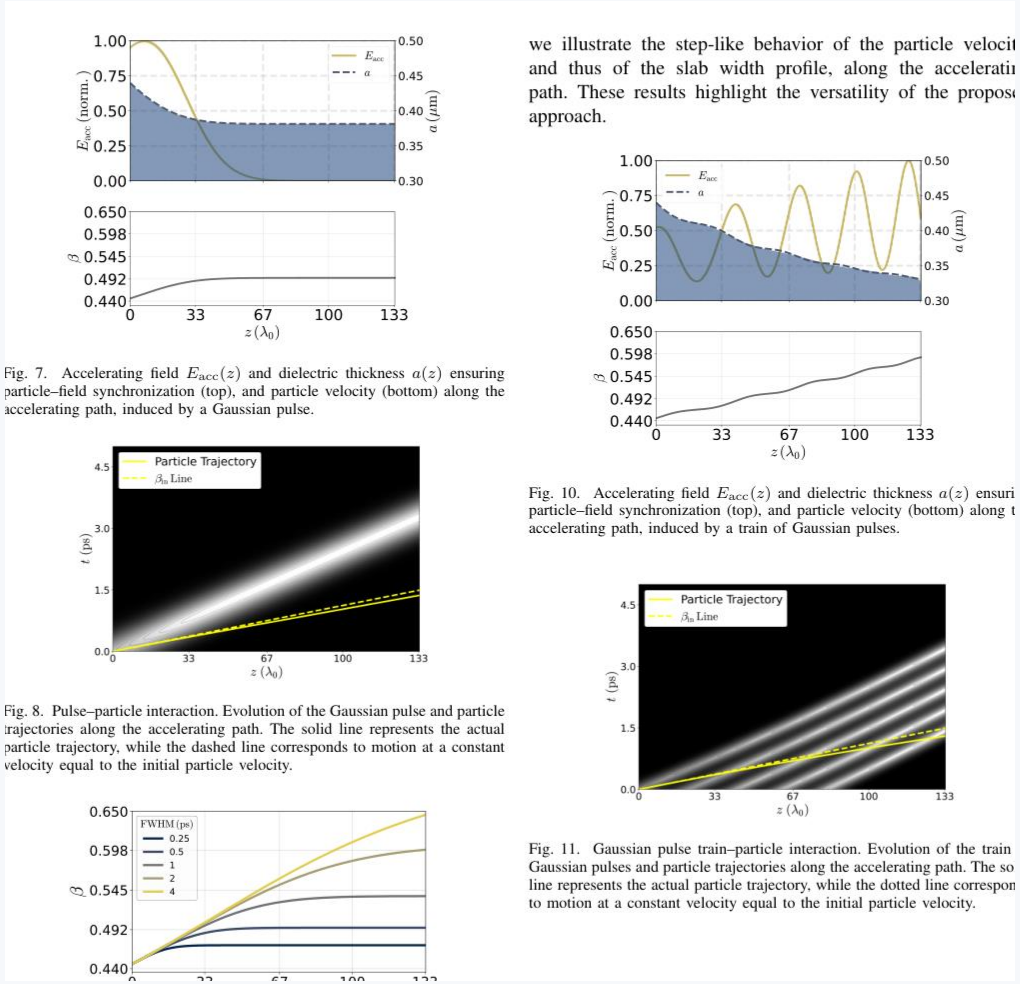
we illustrate the step-like behavior of the particle velocit
and thus of the slab width profile, along the acceleratin
path. These results highlight the versatility of the propos
approach.

Fig. 7. Accelerating field $E_{\mathrm{acc}}(z)$ and dielectric thickness $a(z)$ ensuring particle–field synchronization (top), and particle velocity (bottom) along the accelerating path, induced by a Gaussian pulse.

Fig. 8. Pulse–particle interaction. Evolution of the Gaussian pulse and particle trajectories along the accelerating path. The solid line represents the actual particle trajectory, while the dashed line corresponds to motion at a constant velocity equal to the initial particle velocity.

Fig. 10. Accelerating field $E_{\mathrm{acc}}(z)$ and dielectric thickness $a(z)$ ensuri
particle–field synchronization (top), and particle velocity (bottom) along t
accelerating path, induced by a train of Gaussian pulses.

Fig. 11. Gaussian pulse train–particle interaction. Evolution of the train
Gaussian pulses and particle trajectories along the accelerating path. The so
line represents the actual particle trajectory, while the dotted line correspon
to motion at a constant velocity equal to the initial particle velocity.

D. Guarnera et al., manuscript in preparation (2026).

Practical meaning

Shorter pulse → higher peak field but shorter useful overlap.

Longer pulse → better overlap but lower peak intensity for fixed energy.

Pulse trains can restore interaction regions while keeping fs-scale fields.

PULSE MODEL

With a finite laser pulse, the taper is optimized for the actual pulse envelope sampled by the electron — not for an ideal CW field.

1. Geometry / modal calibration

- local geometry $a(z)$
- $v_{ph}(a)$: phase velocity
- $v_g(a)$: group velocity
- $k_2(a)$: group-velocity dispersion
- $k_3(a)$: third-order dispersion
- $\alpha(a)$: taper-induced amplitude / loss term

all read from local mode calibration

2. Pulse-envelope propagation

- propagate $A(z,t)$ with fast BPM
- envelope walk-off depends on v_g
- pulse broadening from k_2
- pulse asymmetry from k_3
- amplitude changes from α

3. Field sampled by the electron

- $E_{acc}(z,t_z)$ is the actual pulsed field
- the electron samples a moving envelope
- finite overlap limits useful interaction length

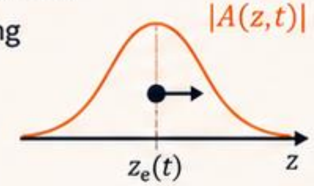

4. Particle dynamics

- update $p(z)$, $W(z)$, $\beta(z)$
- electron velocity changes during acceleration
- particle can outrun or lag the pulse envelope

5. Taper update

- choose $a(z+\Delta z)$
- enforce carrier synchronism: $v_{ph}[a(z+\Delta z)] = v_p(z+\Delta z)$
- but using the pulsed field from the previous steps
- output: self-consistent taper profile

Self-consistent loop

pulse propagation + particle dynamics + taper update

What are k_2, k_3, α?

k_2: pulse broadening (group-velocity dispersion)

k_3: pulse asymmetry / higher-order dispersion

α: gradual field-amplitude change due to taper / loss

In pulsed operation the taper is optimized considering the finite pulse envelope, dispersion, walk-off, and the actual field experienced by the electron.

Part II — Pulsed operation

The CW design optimizes only the phase velocity.

Phase matching is necessary, but in pulsed operation the useful acceleration length is set by envelope walk-off and dispersion

Our pulsed model solves self-consistently the propagation of the optical pulse, dispersion, envelope walk-off, particle dynamics and taper evolution.

As a result, the taper is optimized for the actual field experienced by the electron, not for an ideal continuous-wave field.

Part III — Hollow-core photonic crystal waveguides

A second structural branch to bridge from $\beta \approx 0.7$ toward $\beta = 1$.

Multi-stage velocity-matched architecture

→ enables scalable, phase-synchronized acceleration

We consider different regimes based on particle velocity β*=vp/c:*

- **Slot waveguide** [0.4<β<0.65]

- **Photonic Crystal (PhC) waveguide** [0.7<β<1]

- **Woodpile** [β=1]

Hollow-core PhC waveguide for $\beta \approx 0.7 \rightarrow 1$

A triangular lattice creates a bandgap;

- triangular lattice → **bandgap**

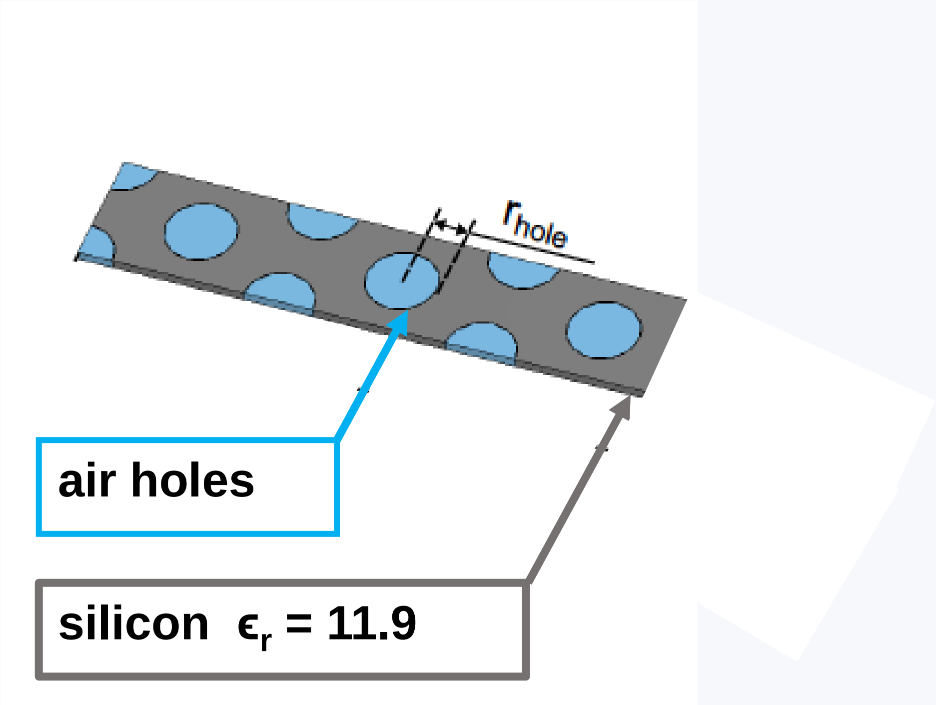

Operating point: confined TM_{01}-like mode, with longitudinal E_z dominant in the hollow channel.

G. S. Mauro et al., "Design of a Tapered Triangular-Lattice Hollow-Core PhC Waveguide," manuscript in preparation (2026).

Photonic Crystal Waveguide supercell for Acceleration

A triangular lattice creates a bandgap; a central defect traps a TM-like accelerating mode.

- triangular lattice → **bandgap**
- central defect → **waveguide**

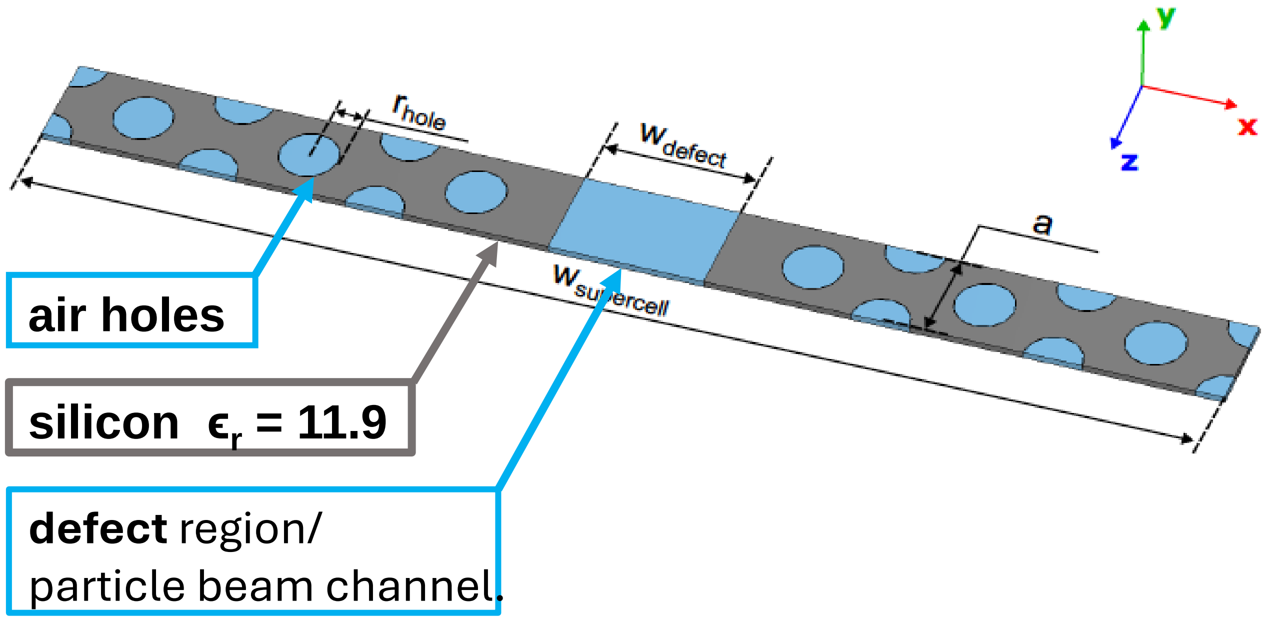

Band Diagram & Operating Point

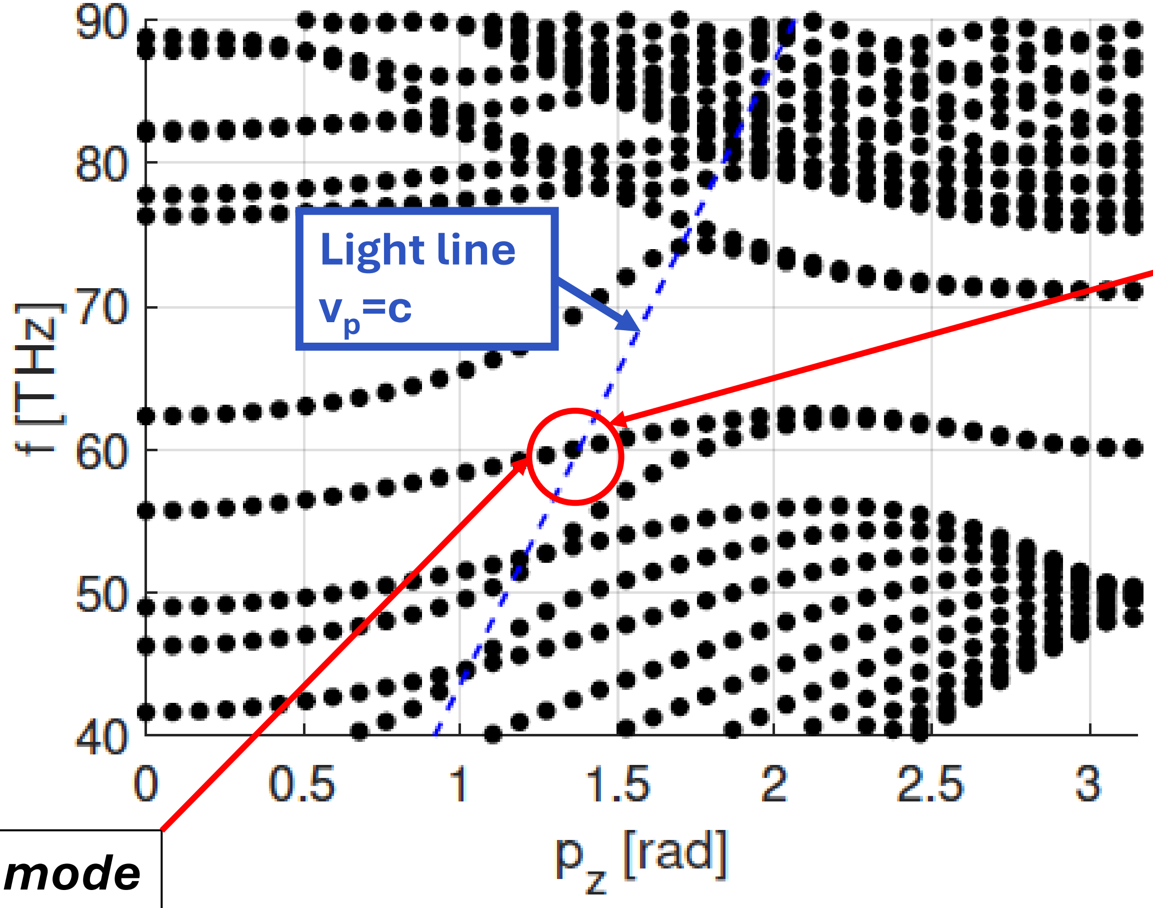

Intersection @ f_0 between the synchronous mode and the light line

At this frequency, the mode becomes synchronous with relativistic electrons.

2D photonic crystal waveguide design procedure

a) computation of the **band diagram** of the triangular lattice primitive cell

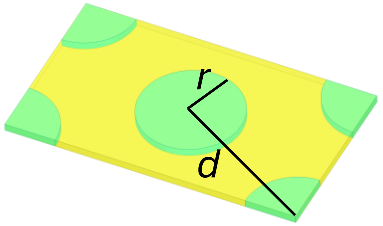

b) computation of the **projected band diagram** of a triangular lattice supercell

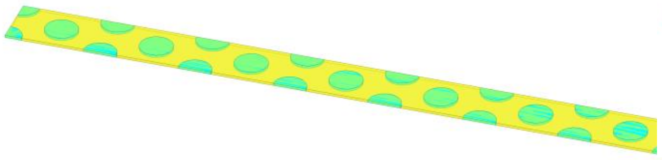

c) add a **hollow-core linear defect** to the supercell

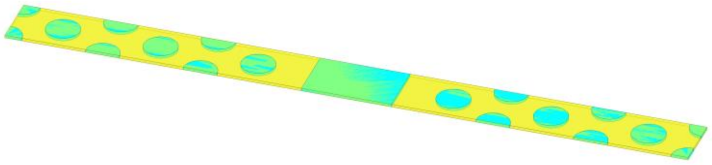

Creating the Accelerating Waveguide

2D photonic crystal waveguide design procedure

a) computation of the **band diagram** of the triangular lattice primitive cell

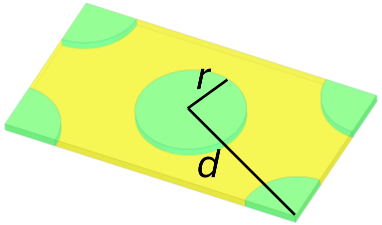

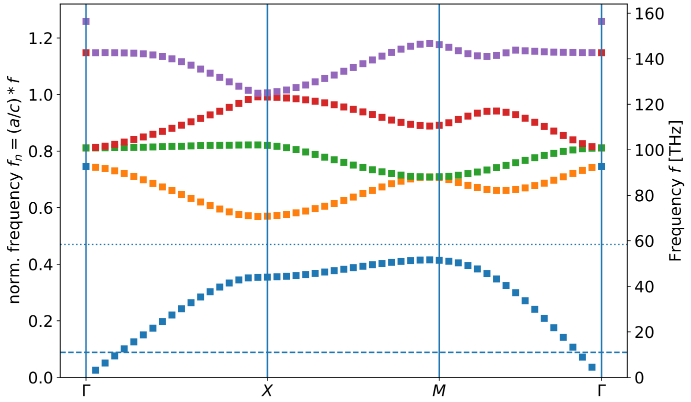

b) computation of the **projected band diagram** of a triangular lattice supercell

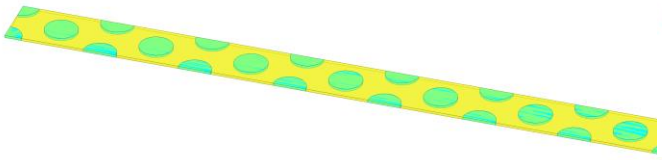

c) add a **hollow-core linear defect** to the supercell

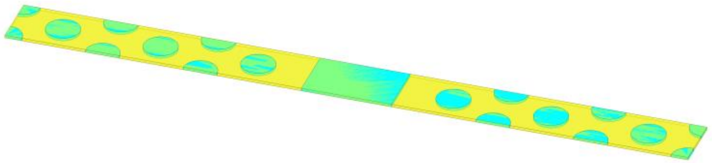

Creating the Accelerating Waveguide

2D photonic crystal waveguide design procedure

a) computation of the **band diagram** of the triangular lattice primitive cell

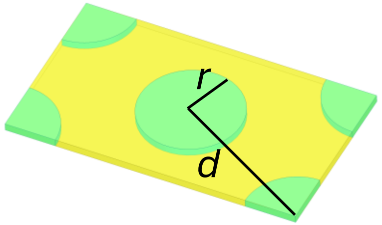

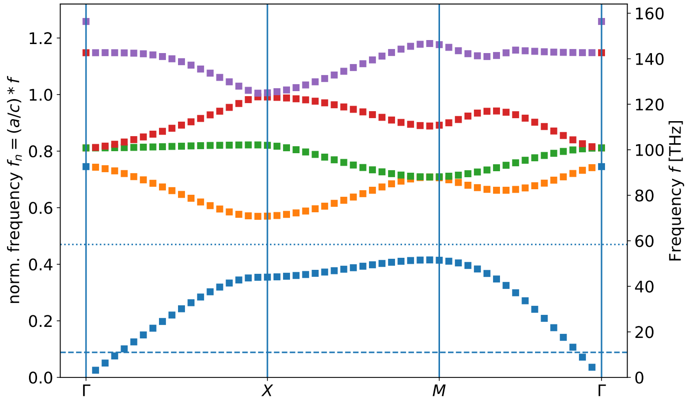

b) computation of the **projected band diagram** of a triangular lattice supercell

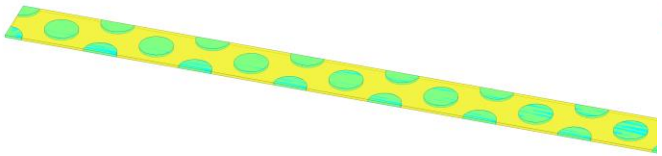

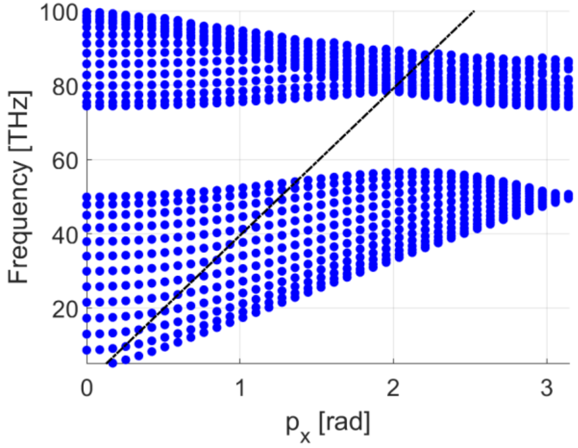

c) add a **hollow-core linear defect** to the supercell

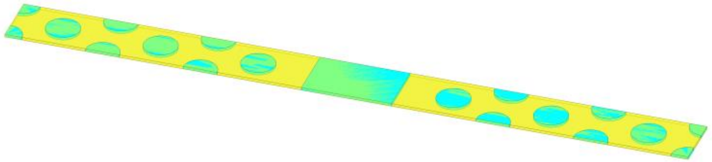

Creating the Accelerating Waveguide

2D photonic crystal waveguide design procedure

a) computation of the **band diagram** of the triangular lattice primitive cell

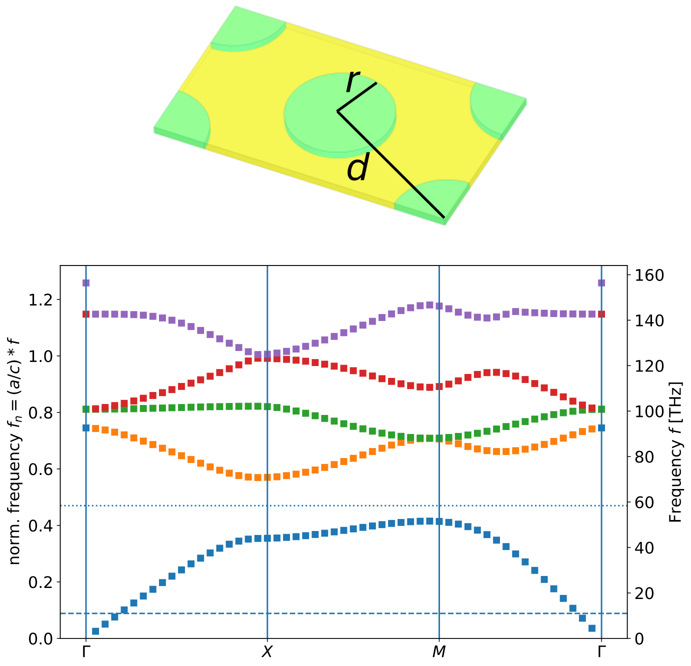

b) computation of the **projected band diagram** of a triangular lattice supercell

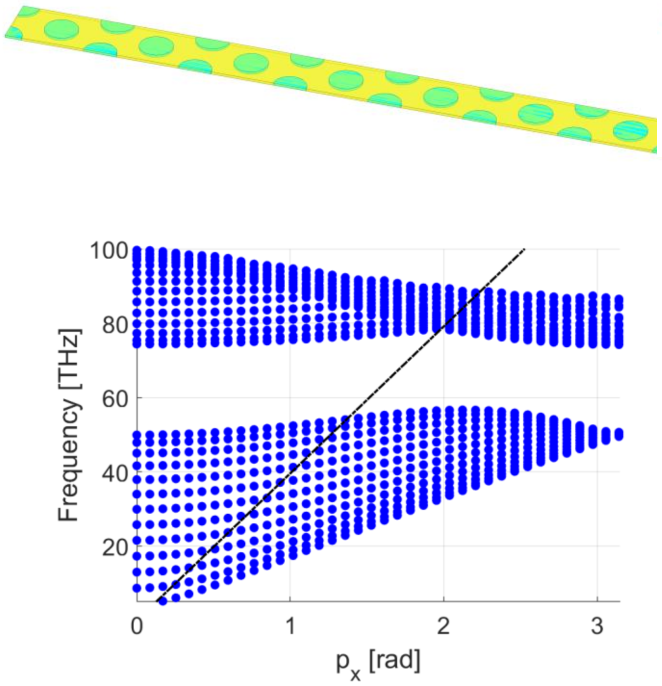

c) add a **hollow-core linear defect** to the supercell

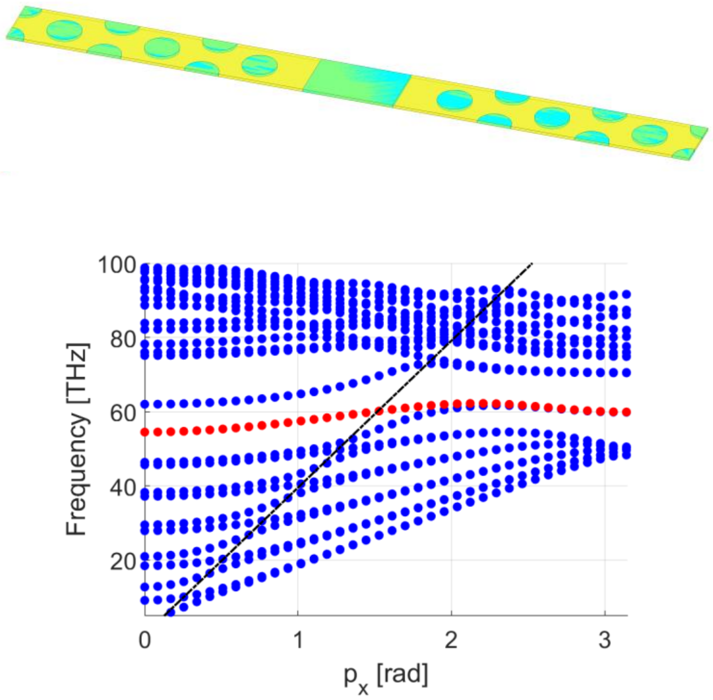

Creating the Accelerating Waveguide

2D photonic crystal waveguide

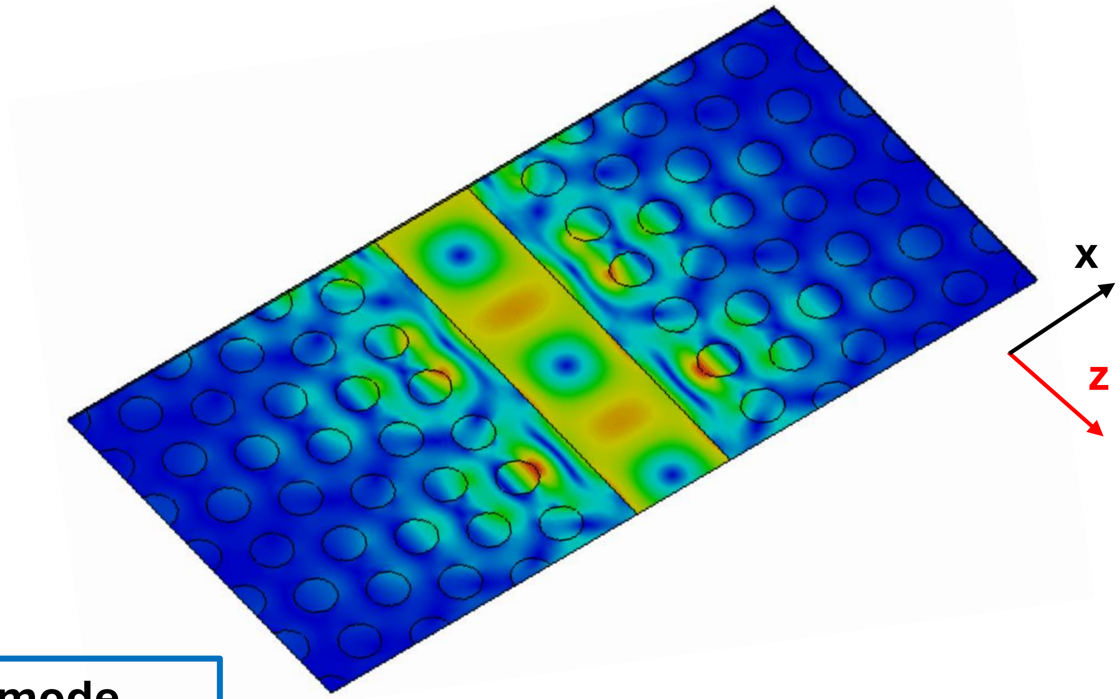

Confined TM01-like mode

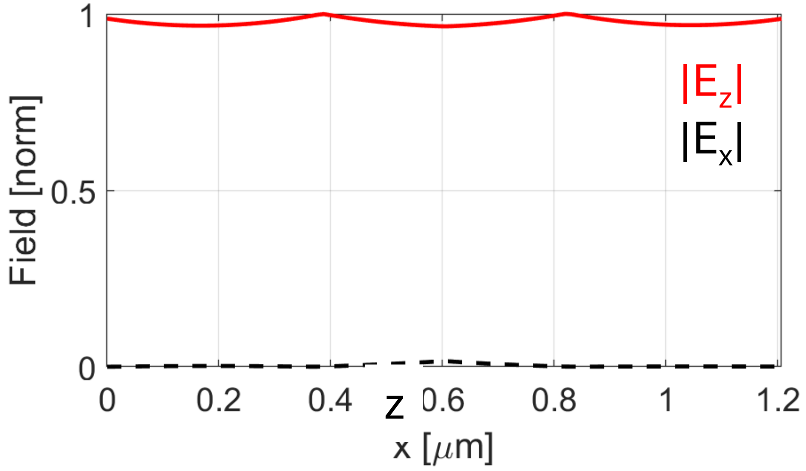

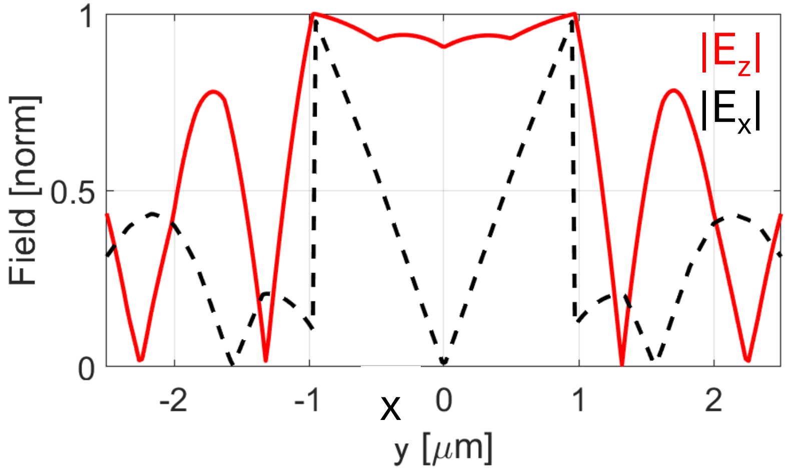

Phase of E_z along z vs. $\frac{\omega}{c}z$

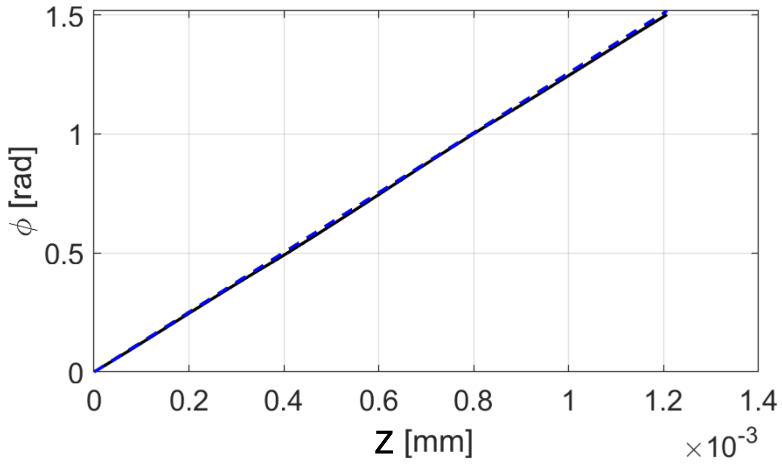

2D photonic crystal waveguide

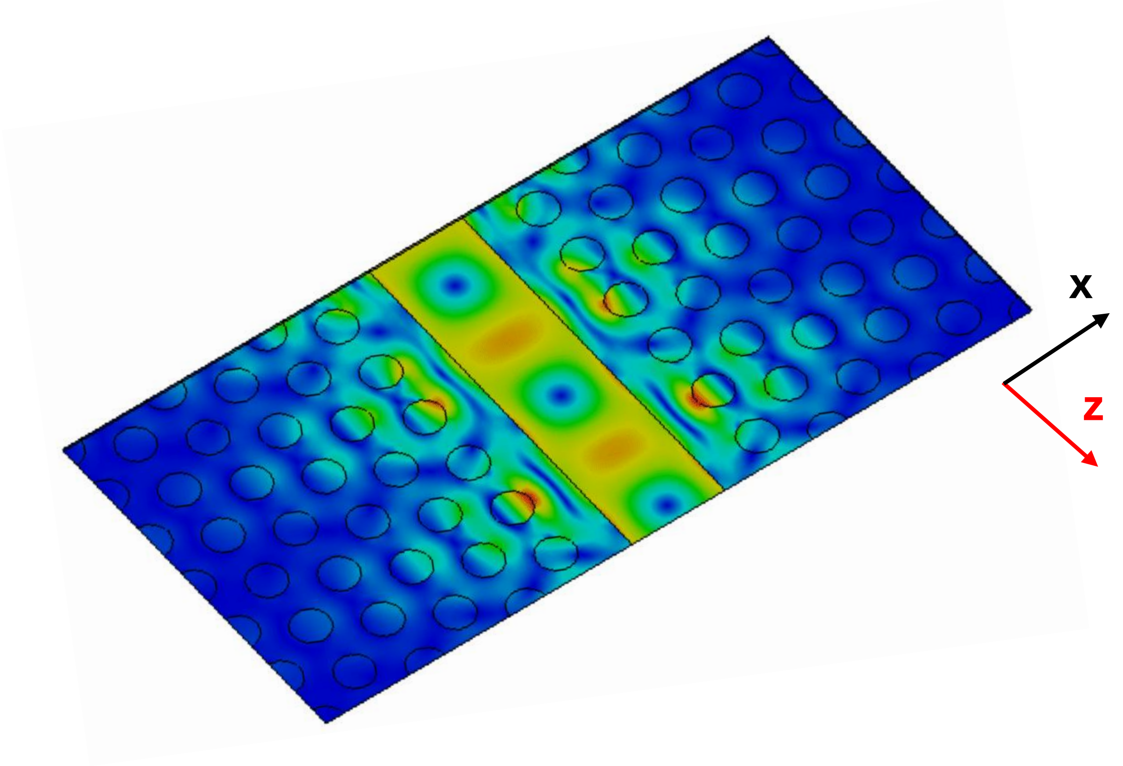

- the structure supports a confined TM-like accelerating mode

- How do we control the phase velocity to match the particle?

Tuning Phase Velocity via Defect Width

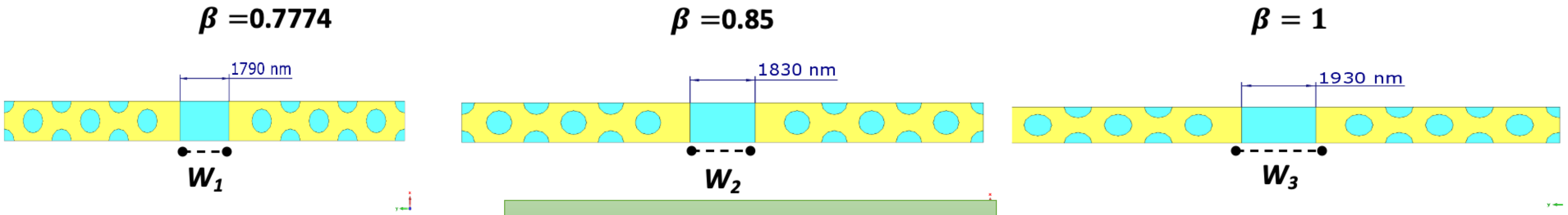

Increasing W → Increasing β

Tuning Phase Velocity via Defect Width

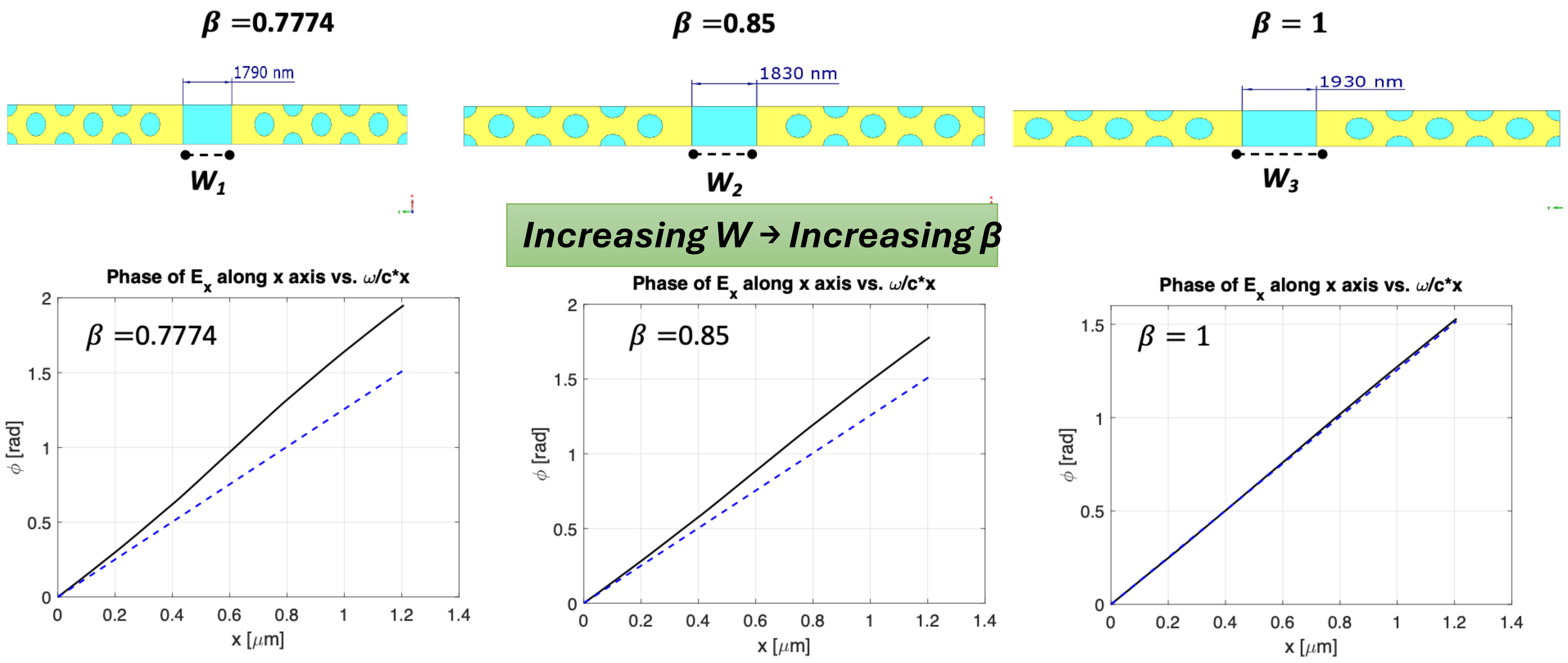

Adiabatic Taper for continuous Phase Matching

parametrized taper by a progressive shift of the lattice

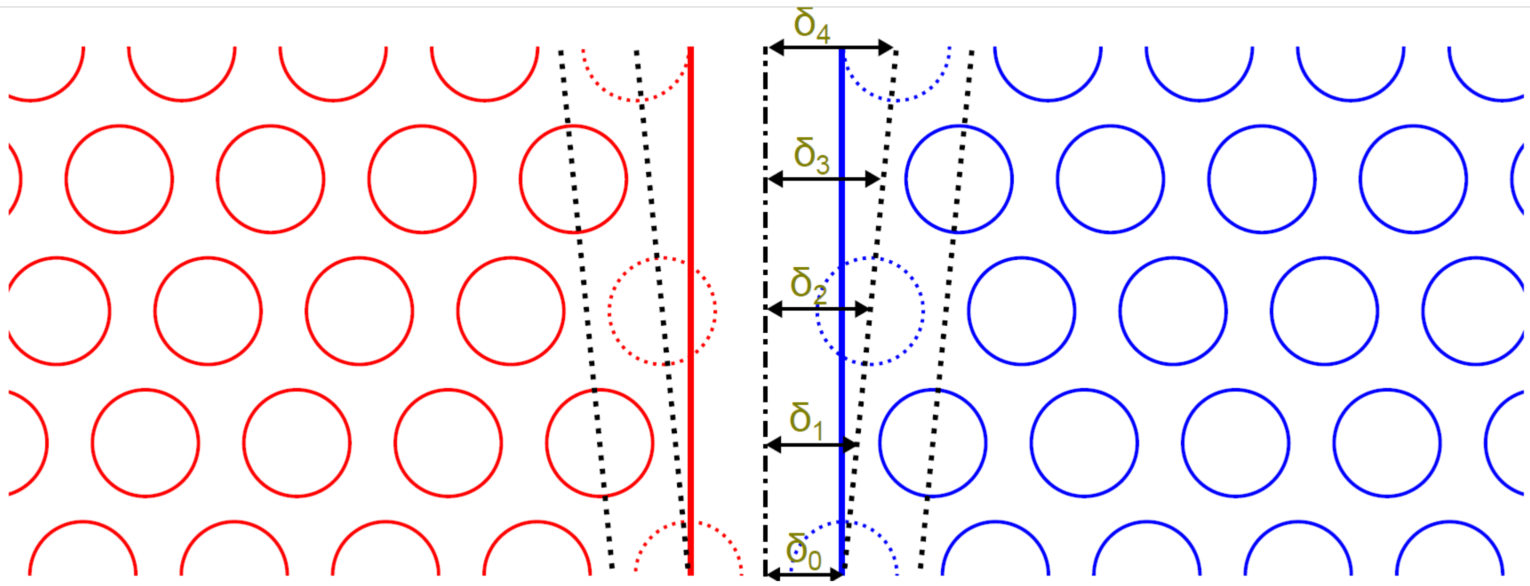

Structure adapts to keep phase synchronism

➢**shift of the air rods along the transversal direction.**

$$\delta_i = \frac{i}{N}\frac{w_p}{2}$$

- N is fixed by the taper length
- w_p is the padding width to obtain a specific β

Confined Accelerating Mode

Eigenmode Simulation

nearby rods are shifted to tune the guided mode.

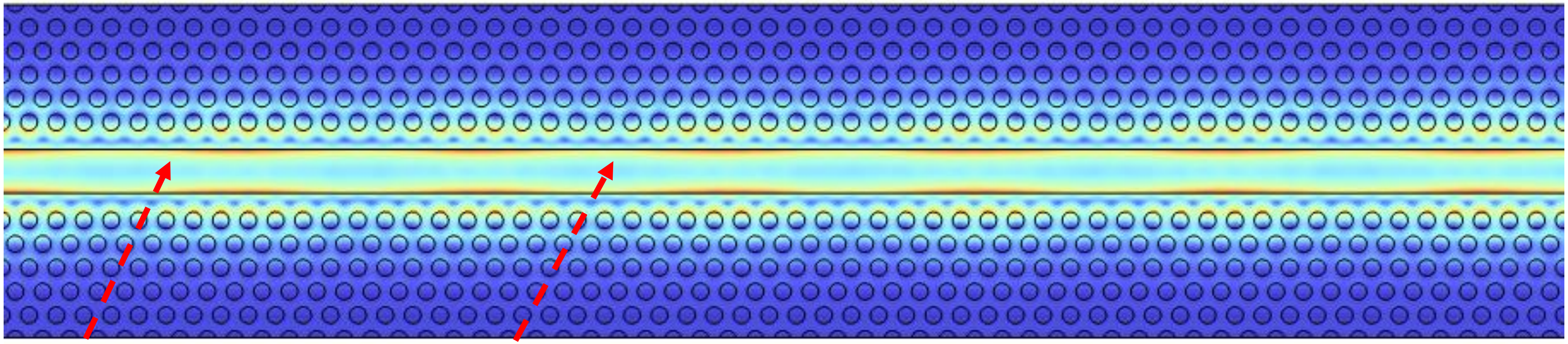

Hollow-core channel

Strong E_z field

G. S. Mauro et al., “Design of a Tapered Triangular-Lattice Hollow-Core PhC Waveguide,” manuscript in preparation (2026).

Longitudinal Field Dominates

Ez >> Ex

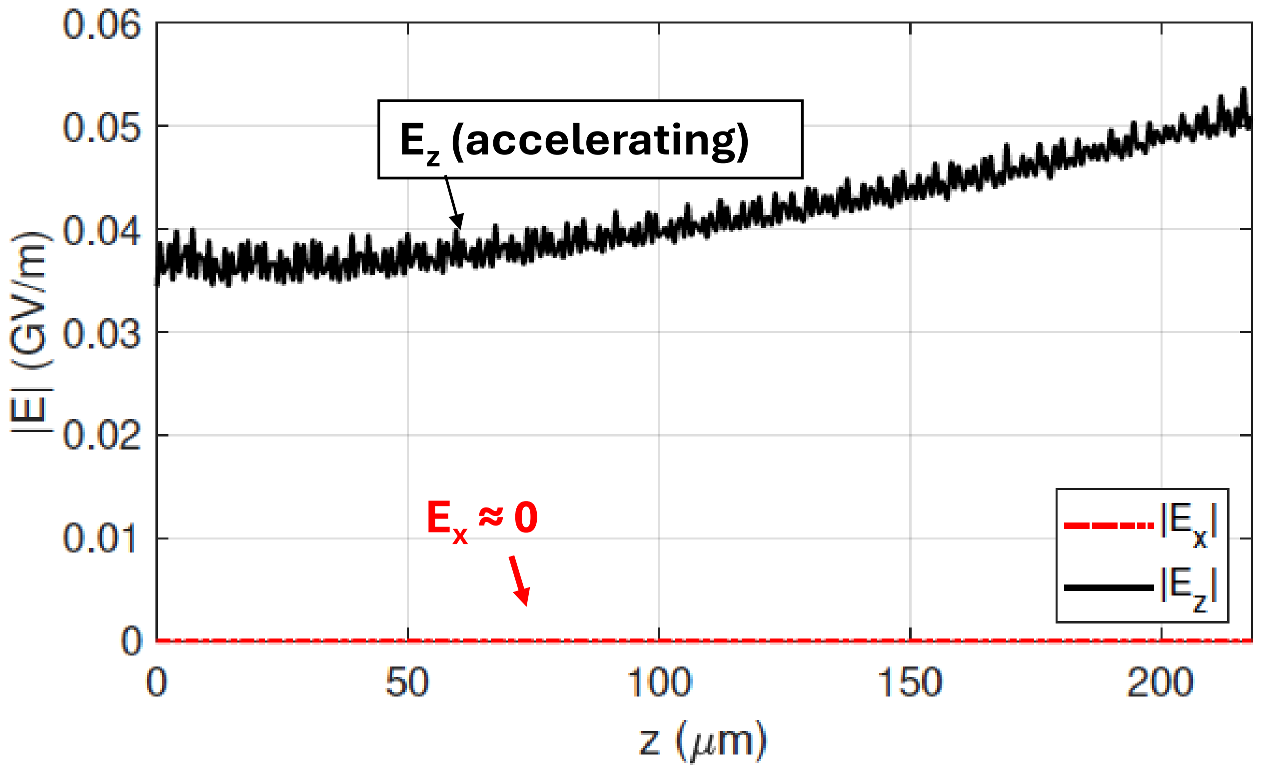

Phase Adaptation Along the Taper

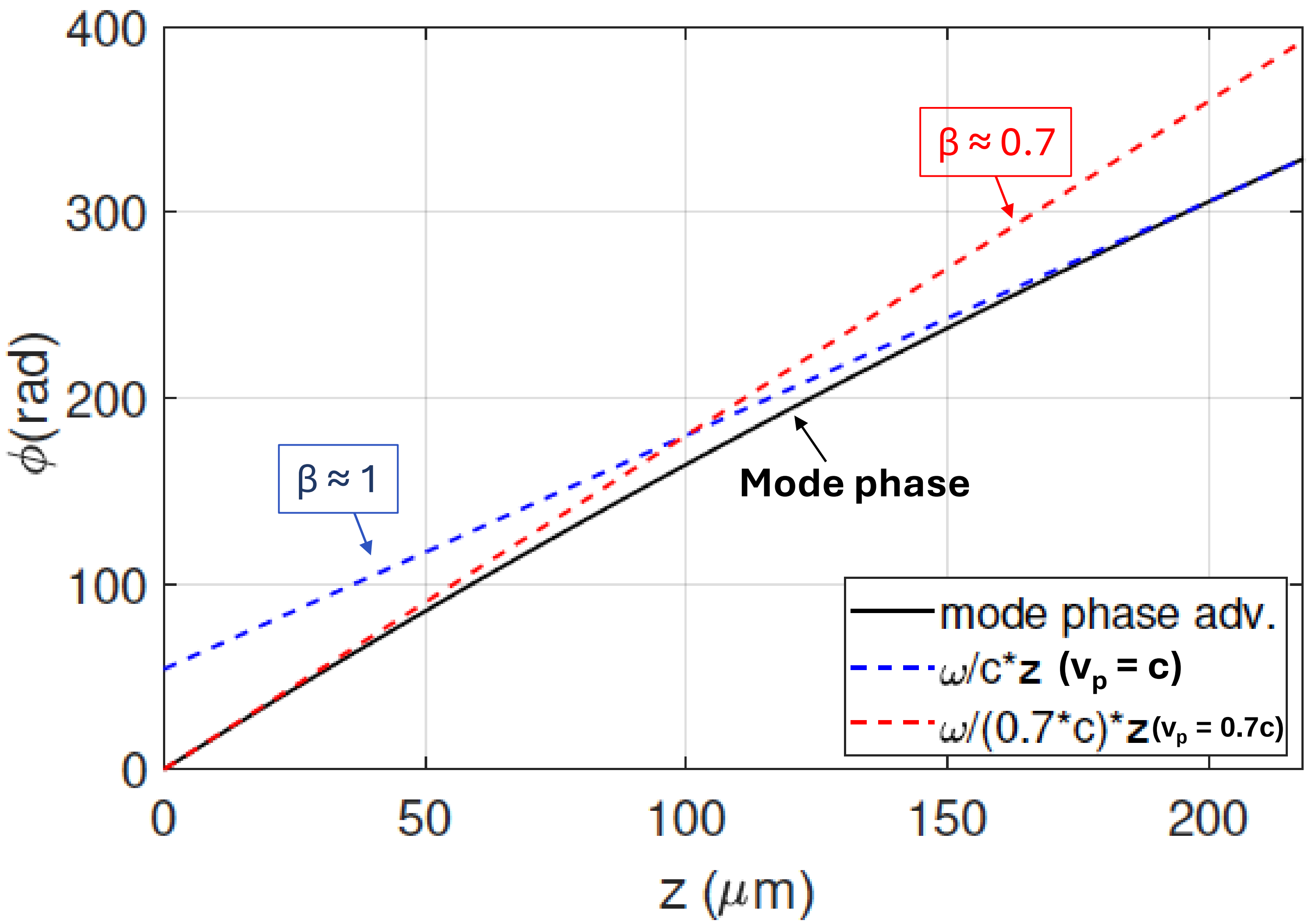

Driven validation: side-coupler and TM-like mode conversion

- Tapered waveguide with $\boldsymbol{\beta}$=[$\mathbf{0.7}$, $\mathbf{0.84}$], feeded by a 90-deg I/O side coupler.

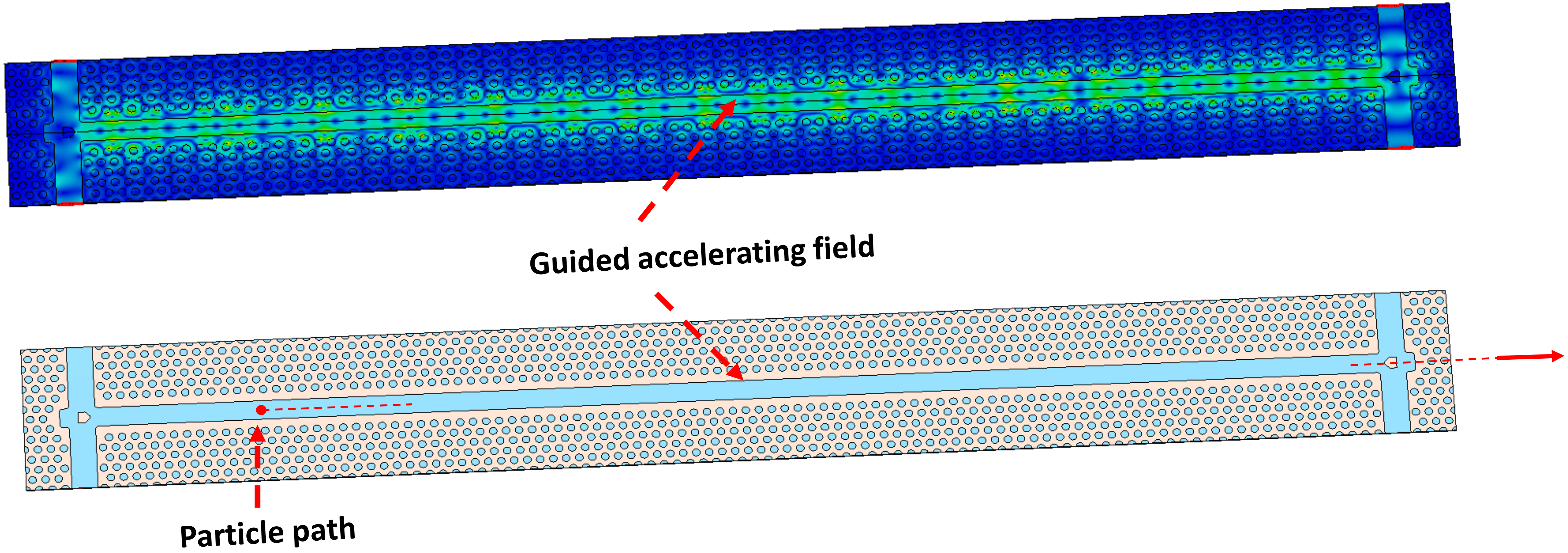

G. S. Mauro et al., "Design of a Tapered Triangular-Lattice Hollow-Core PhC Waveguide," manuscript in preparation (2026).

Driven validation: side-coupler and TM-like mode conversion

- Tapered waveguide with $\boldsymbol{\beta}=[\mathbf{0.7}, \mathbf{0.84}]$, feeded by a 90-deg I/O side coupler.

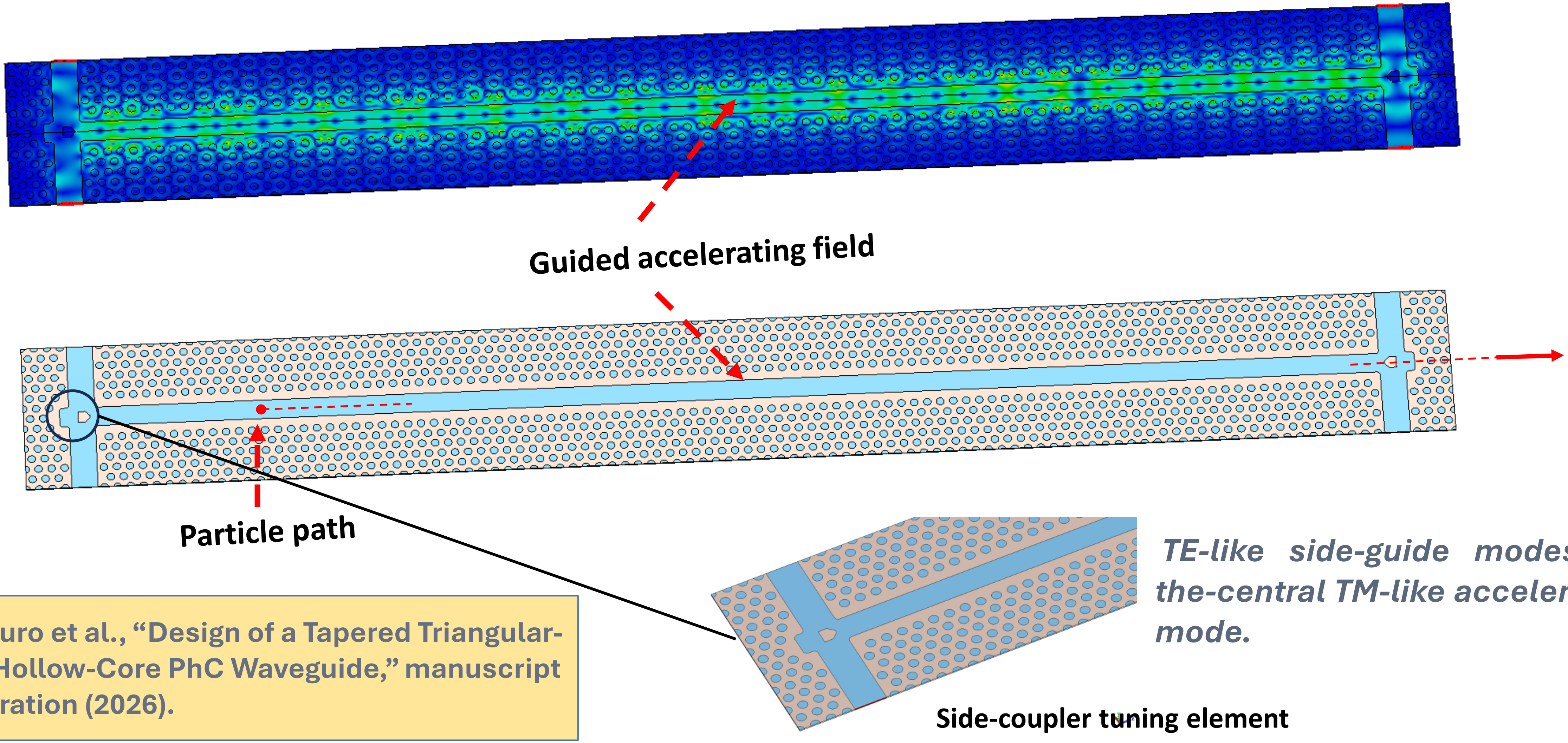

TE-like side-guide modes to-the-central TM-like accelerating mode.

G. S. Mauro et al., "Design of a Tapered Triangular-Lattice Hollow-Core PhC Waveguide," manuscript in preparation (2026).

Driven Response

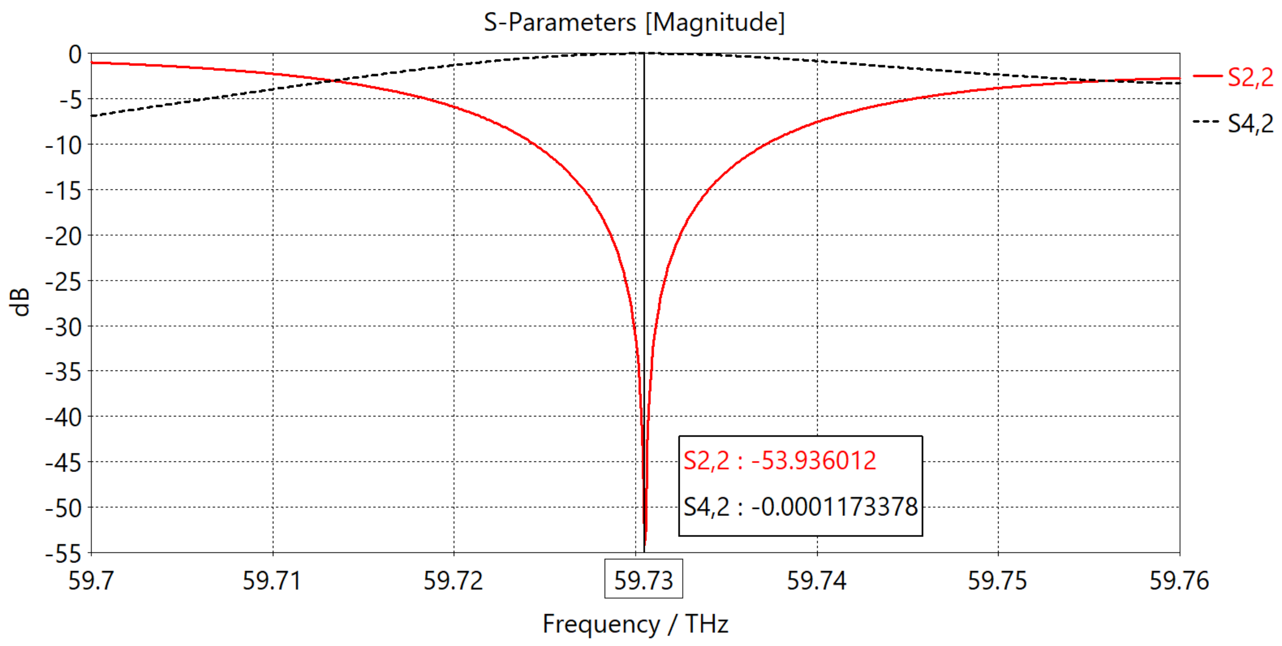

Field and Phase Consistency

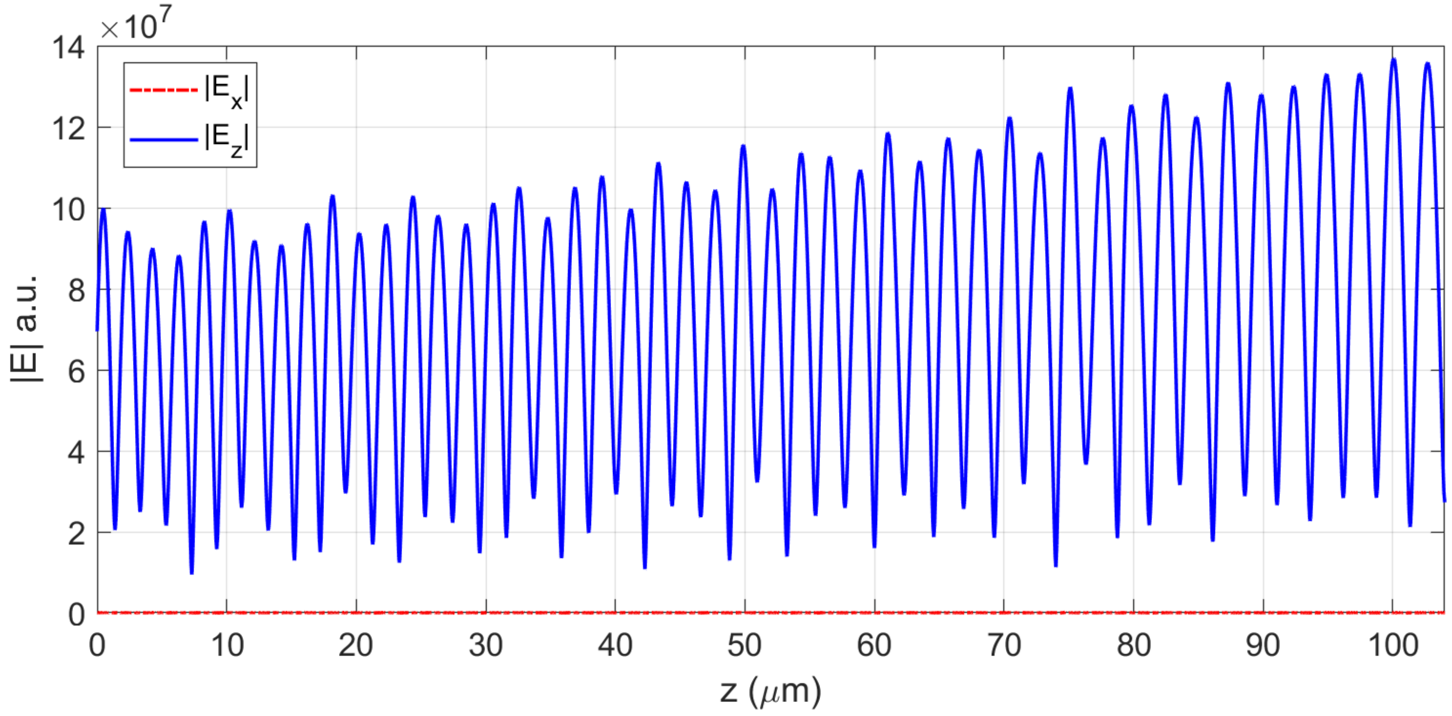

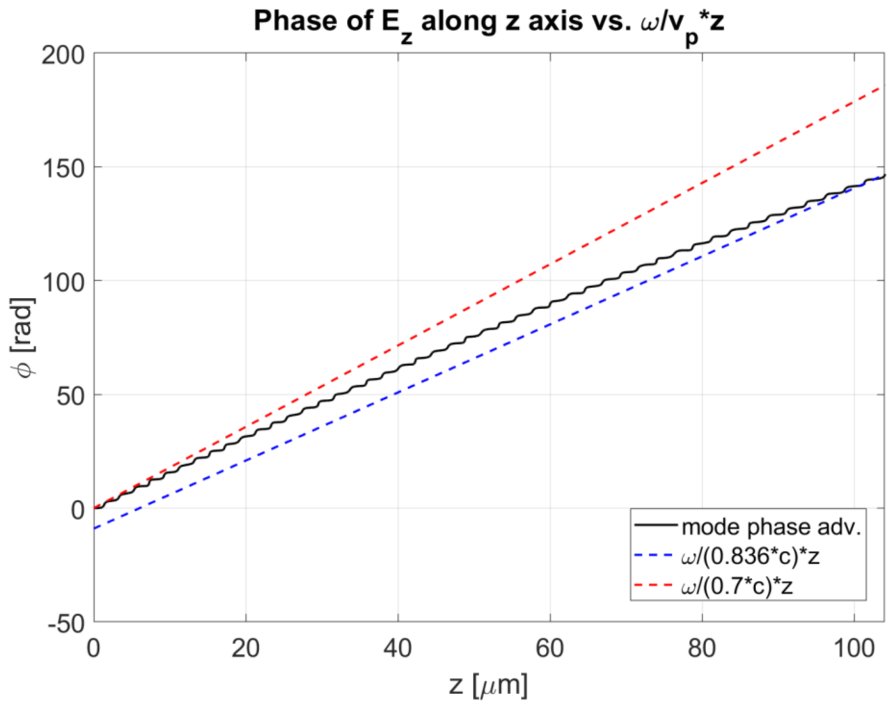

Fabrication of the Slot waveguide (INFN-Torino, CNR, INRIM and CNRS-C2N)

fabrication feedback

- SOI stack tests initially considered
- device-layer thickness tolerance can be limiting
- a-Si deposition on SiO_2 may give better process control
- thermal conductivity and optical losses remain to be tested

Fabrication of the Slot waveguide (INFN-Torino, CNR, INRIM)

- The work has been focused on **Si on SiO2 stack tests in order to identify the optimal process**.
- The goal is to print the first selected accelerating structure, the slot waveguide (λ = 2 μm).

- **Displayed Width:** 5000 nm
- **Layer 1:** SiO2
- **Thickness:** 2 μm
- **Layer 2:** Si
- **Thickness:** 500 μm
- **Layer 3:** SiO2
- **Thickness:** 2 μm
- **Layer 4:** Si
- **Thickness:** 2 μm

- Starting from a commercial structure, the goal was to try to etch some thickness to layer 4 in order to get to the wanted thickness for the structure (250 nm).
- Etch results: the tollerance in the device layer thickness (± 10%) do not allow for a good control of the final Si layer thickness.

Fabrication of the Slot waveguide (INFN-Torino, CNR, INRIM)

- Solution: avoid etching the Si of the layer given by the supplier and make the two waveguides by Si deposition on the SiO2 layer 3.

- This way can be pursued by using amorphus Si (instead of polycristalline Si). This shall not impact on the material electric properties (ε_r, $tang\delta$).

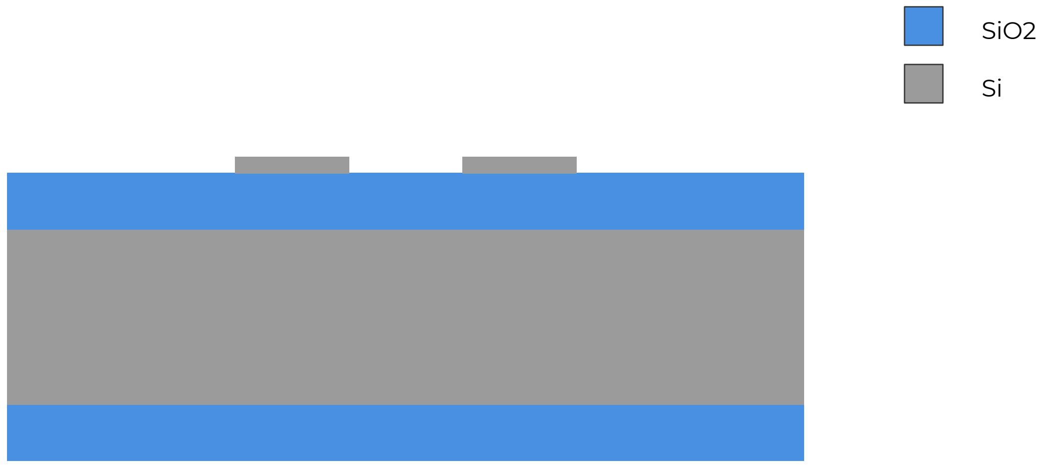

SLOT WAVEGUIDE Fabrication (CNRS/C2N)
reality check: nm-scale tapering

CNRS/C2N processed an INFN slot-waveguide test with a nominal width variation of only 3 nm

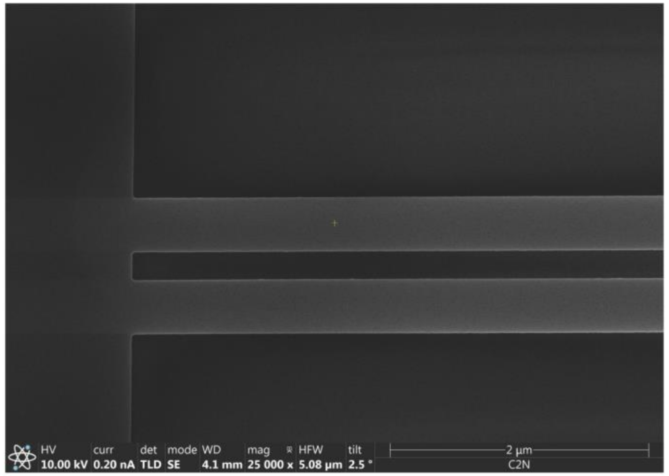

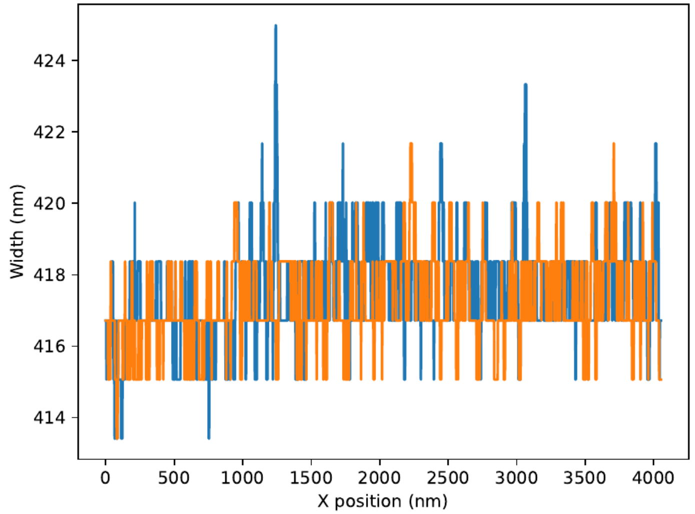

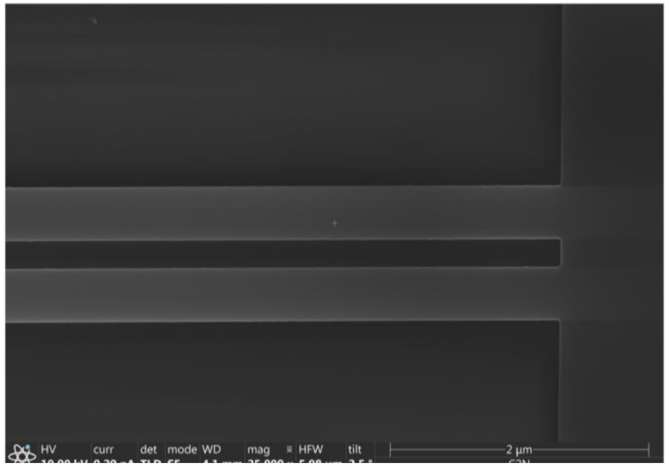

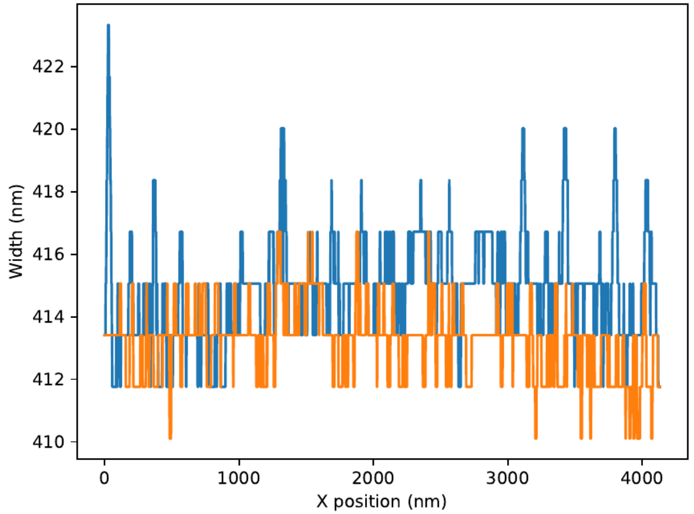

Key numbers

- SOI: 220 nm Si on 2 µm SiO_2
- 100 keV EBL, positive ZEP resist
- standard ICP etch; no Si smoothing
- measured width difference ≈ 2.7–3.0 nm

Conclusion: 3 nm variation is processable and measurable; roughness must still be improved.

Part IV — Experimental coupling strategy

A realistic route from optical to accelerating-mode validation.

Experimental strategy at 2 μm

1 **End-fire / cut-back**

T(λ), cutoff, propagation loss α(λ), converter loss

2 **Two-arm phase-controlled coupling**

grating efficiency, Δϕ=0/π, mode selection

3 **Future pulsed DLA roadmap**

Satsuma pump → OPA/OPG at 2 μm, fs diagnostics, e-beam integration

INFN-LNS laser roadmap: Satsuma is the first-light platform

The 1030 nm system is operational

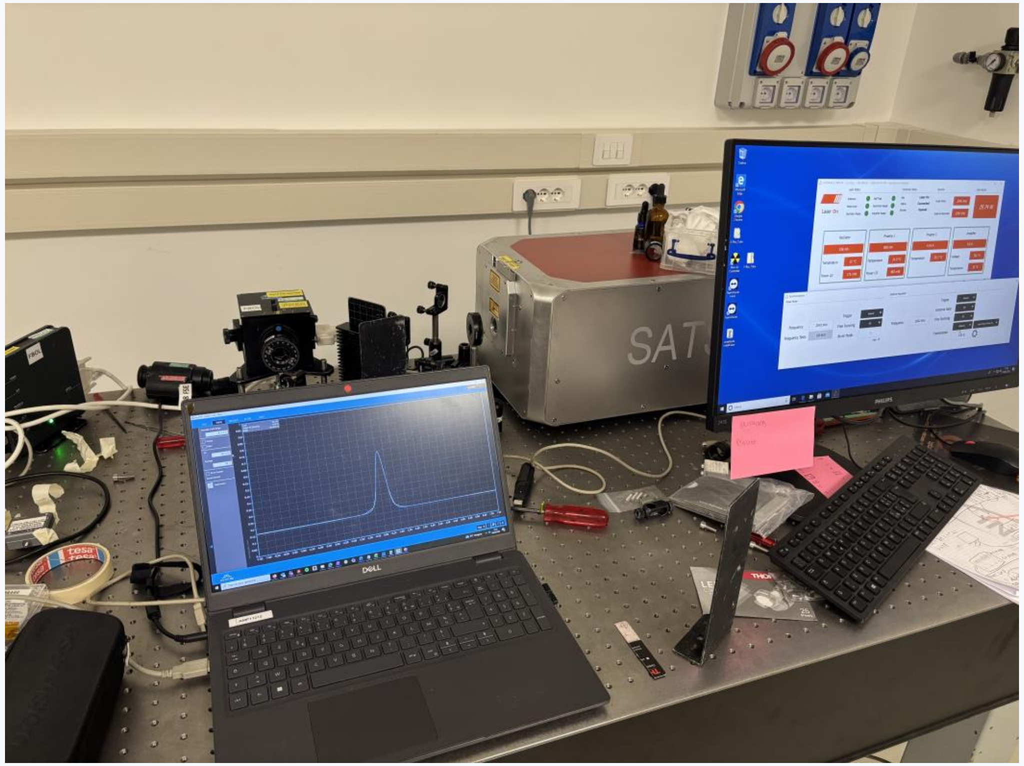

Satsuma X-28 available at LNS

- 1030 nm source: first-light and pump laser
- ~420 fs pulses, ~30 W average power class
- 2 µm DLA test requires OPA/OPG or equivalent source

- The 1030 nm Satsuma X-28 is installed, commissioned and already usable for first-light work.
- The acceptance report confirms sub-500 fs pulses, about 30 W average power, and excellent 11.3 h power stability.
- For the DLA experiment, the key point is that this is the near-term beam-delivery and diagnostics platform;

EPITA context

WP5 laser-driven acceleration is one of the EPITA technology areas.

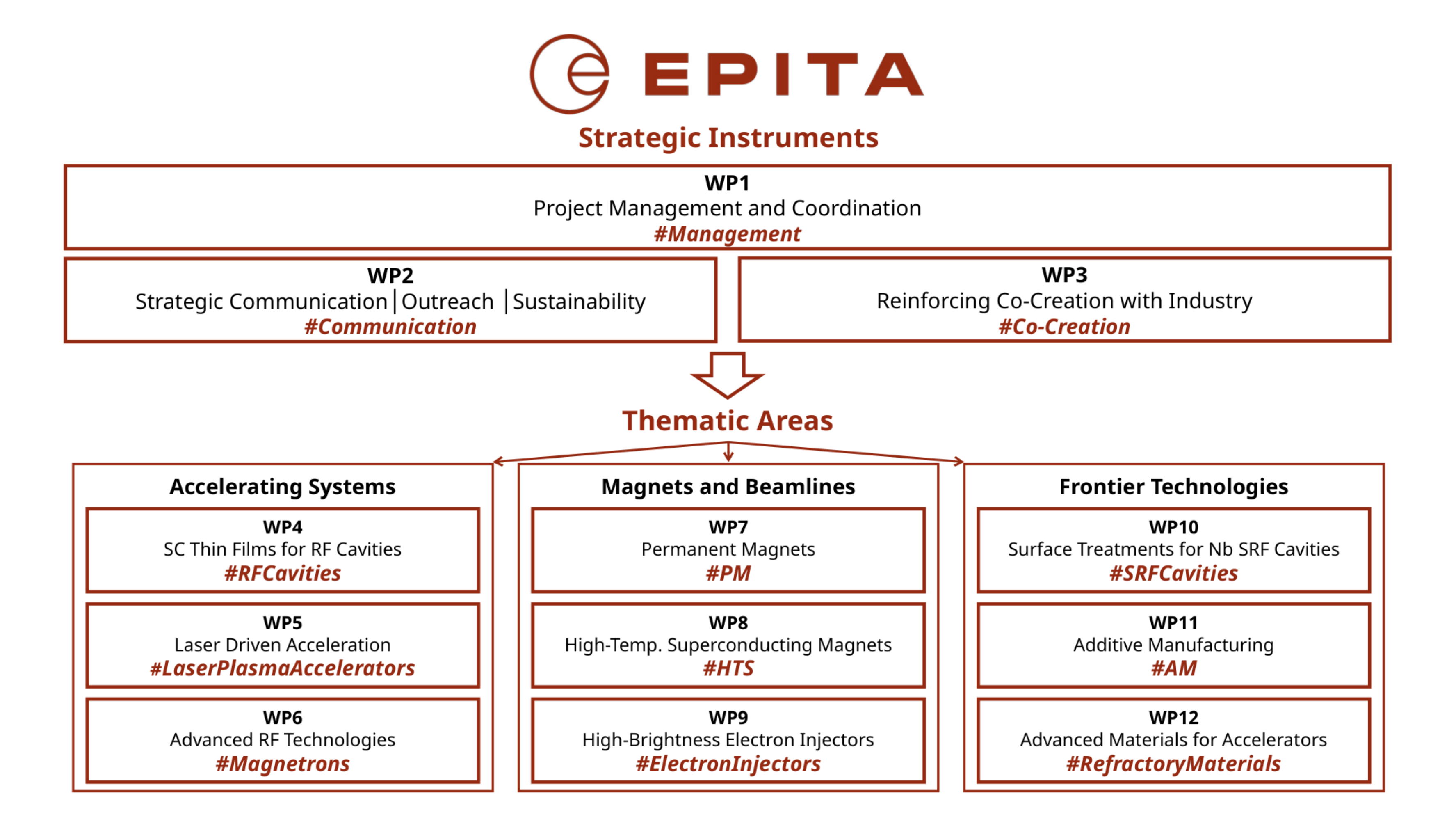

INFN-iDLA and EU-HE-EPITA: from design to prototype and test

The activity is embedded in INFN CSN5 and in the European WP5 laser-driven acceleration roadmap.

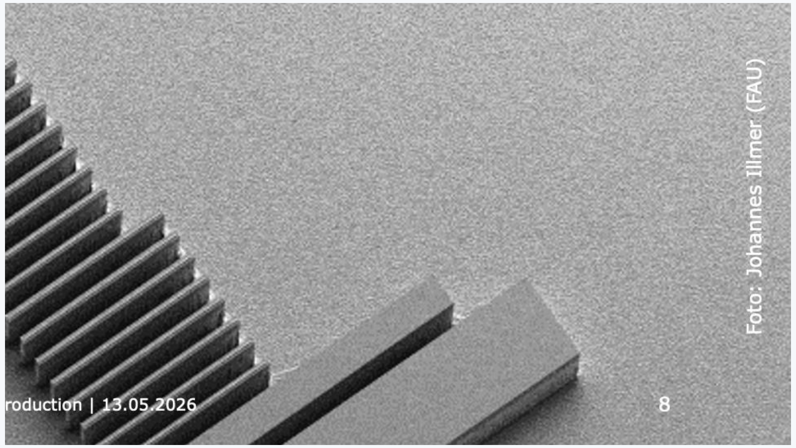

[from EPITA WP5 introduction slides, A. Maier (DESY), 13.05.2026]

EPITA WP5 — Task 5.5

Co-propagating DLA structure

Partners
INFN/LNS, PSI, FAU/LMU, SENSIC

Prototype goal:
enhanced DLA performance through co-propagating dielectric structure

Conclusion

1

Phase matching engineered

For sub-relativistic electrons, β changes and the structure must adapt.

2

Co-propagation offers a scaling route

Slot and hollow-core PhC structures provide guided interaction along the beam path.

3

Real operation requires coupled modeling and experiments

Pulses, fabrication, coupling and beam dynamics must be designed together.

Co-propagating hybrid tunable phase-matched structures are a realistic path from local high gradients to controlled energy gain.

Co-propagating Dielectric Laser Accelerators for compact high-gradient particle acceleration

INFN
LNS
Istituto Nazionale di Fisica Nucleare
Laboratori Nazionali del Sud

Thank you

Giuseppe Torrisi • *INFN–LNS, Catania, Italy*
G. S. Mauro, D. Mascali ***(INFN-LNS),*** A. Bacci ***(INFN-Milano)***
R. Palmeri ***(UniRC)***, A. Locatelli ***(UniBS)***, L. Vincetti ***(UniMoRe)***, G. Sorbello ***(UniCT)***